# Blind User Identification in a Chip-Synchronous CDMA System

Afshin Haghighat

A Thesis

in

The Department

of

Electrical and Computer Engineering

Presented in Partial Fulfillment of the Requirements
for the Degree of Doctor of Philosophy (Ph.D.) at
Concordia University
Montreal, Quebec, Canada

April 2005

*Your file Votre référence*
*ISBN: 0-494-04057-2*
*Our file Notre référence*
*ISBN: 0-494-04057-2*

# Abstract

*Blind User Identification in a Chip-Synchronous CDMA System*

Afshin Haghighat, Ph.D.

Concordia University, 2005

User identification provides valuable information about the active users in a Code Division Multiple Access (CDMA) system that could be used in numerous applications. Most importantly, it can produce a reliable estimate of multiple access interference, whose cancellation is the main objective of multiuser detection schemes. Several schemes have been introduced for user identification in a synchronous CDMA system. The main distinguishing factor between different user identification schemes is the amount of information about each user required to be available in advance at the receiver. The existing schemes require prior knowledge of users' spreading codes or some other forms of assistance. However, the proposed method does not need the prior knowledge of the spreading codes nor relies on any assistance. Thus, using the scheme proposed in the thesis, one will be able to perform complete blind identification for a group of users. This identification involves determination of the spreading codes of active users and estimation of their relative timings.

In this thesis, a scheme for blind identification of users in a chip-synchronous Direct Sequence CDMA (DS-CDMA) system is presented. The proposed approach is based on the subspace decomposition and searches for a solution that minimizes a defined cost function. The search is performed over both signal space and time domain. By completing the identification of the users, other important parameters such as user timings and power can be evaluated.

Blind identification of users for an asynchronous CDMA system lends itself to several applications such as CDMA up-links, ad-hoc networking, signal interception and non-intrusive tests.

## ACKNOWLEDGEMENTS

I would like to express my sincere gratitude to my thesis advisor, Dr. M. Reza Soleymani for his support and valuable guidance throughout the course of this work.

## *Table of Contents*

## *Chapter 5*

# *List of Figures*

## *List of Tables*

## *List of Symbols*

| | |
|---|---|
| $\mathbf{A}$ | Users' amplitude matrix |
| $A_k$ | Users $k_{th}$ amplitude |
| $\alpha_j$ | Combining factor |
| $\mathbf{b}$ | Vector presentation of the transmitted bits |
| $b_k$ | Users $k_{th}$ transmitted bit |
| $b_i'$ | Estimated bit of the $k_{th}$ user |
| $\mathbf{C}$ | Autocorrelation matrix of the received signal |
| $\mathbf{D}^{p}_{m_k}$ | Permutation matrix |
| $\mathbf{D}^{c}_{m_k}$ | Permutation matrix |
| $\mathbf{d}_i$ | Decorrelator transform |
| $\eta$ | Detection threshold |
| $\mathbf{F}$ | Lower triangular matrix |
| $f_k$ | Signal-Noise projection value |
| $f_{\tilde{J}^{-1}}(\psi)$ | Probability density function |
| $g_k$ | Signal-Signal projection value |
| $\mathbf{\Lambda}$ | General eigenvalue matrix |
| $\mathbf{\Lambda}_n$ | Noise eigenvalue matrix |
| $\mathbf{\Lambda}_s$ | Signal eigenvalue matrix |

| | |
|---|---|
| $\gamma_k^2$ | 2nd order moment of a Rayleigh distribution |
| $\mathbf{I}_N$ | $N \times N$ identity matrix |
| $I_k^{(i-1)}$ | Estimated interference for $k_{th}$ user in the $(i-1)_{st}$ stage |
| $J(\mathbf{d}_i)$ | Cost function |
| K | Number of active users |
| $\lambda_i$ | $i_{th}$ eigenvalue |
| $L_1$ | Accumulation length for autocorrelation matrix |
| $L_2$ | Observation length for inspecting the statistics |
| $\mathbf{M}$ | MMSE detection matrix |
| $\mu_i$ | $i_{th}$ normalizing factor |
| $N$ | Processing gain |
| $\mathbf{n}$ | Vector presentation of the noise |
| $\overline{\mathbf{n}}$ | Noise term after transformation |
| $n(t)$ | Noise term |
| $\mathbf{P}_1$ | Shift-permutation matrix |
| $\mathbf{P}_2$ | Shift-permutation matrix |
| $P_{false}$ | Probability of false detection |
| $P_{miss}$ | Probability of missed detection |
| $p(z_i)$ | Probability density function of the decorrelator output |
| $\varphi_k$ | Channel random phase shift |
| $\mathbf{R}$ | Cross correlation matrix |

| | |
|---|---|
| $\mathbf{r}$ | Vector presentation of the received signal |
| $R_b$ | Bit rate |
| $R_c$ | Chip rate |
| $R_{kj}$ | $kj_{th}$ element of the **R** |
| $r(t)$ | Received signal |
| $\mathbf{S}$ | The whole set of the signature sequences |
| $\mathbf{s}_k$ | Vector presentation of the signature sequence of the $k_{th}$ user |
| $\mathbf{s}_{ki}$ | Effective spreading waveforms in an asynchronous model |
| $s_k(t)$ | Signature sequence of the $k_{th}$ user |
| $\sigma^2$ | Noise variance |
| $\sigma_{A_i}^2$ | Amplitude variance |
| $\sigma_{w_i}^2$ | Noise variance after the decorrelation |
| $\sigma_{z_i}^2$ | Decorrelator output variance |
| $T$ | Bit period |
| $T_c$ | Chip period |
| $\tau_k$ | Delay of user $k_{th}$ |
| $\boldsymbol{\theta}$ | Residual random carrier phase matrix |
| $\theta_k$ | Residual random carrier phase of user $k_{th}$ |
| $\mathbf{U}$ | General eigenvector matrix |
| $\mathbf{U}_n$ | Noise eigenvector matrix |
| $\mathbf{U}_s$ | Signal eigenvector matrix |

| | |
|---|---|
| $\bar{v}$ | Sample variance |
| $w_i$ | Noise term after the decorrelation |
| $\mathbf{y}$ | Detector output |
| $\bar{\mathbf{y}}$ | Detector output after transformation |
| $z_i$ | Decorrelator output |

# *Chapter 1*

# *Introduction*

## *1-1. Background*

Voice transmission has been the driving force in progress and development of cellular wireless systems. However, data services are expected to have significant growth over the next few years and will likely become the dominant source of future generations of wireless system. As the popularity and use of packet-data services increases and new services are introduced, end-users will require higher data rates and improved quality of service (QoS). In order to realize multimedia applications, operators will also require more capacity in their systems. Terminals such as or PDA's (Personal Digital Assistant), smart phones and PCs with high-resolution color screens, larger displays and greater

memory capacity have become more common, requiring greater speed and shorter delays when downloading audio, video and large files, or playing games.

The personal mobile wireless systems currently in use around the world are first, second and third generation systems. First generation systems consist of the analog mobile phones that offered only voice communications, like Advanced Mobile Phone System (AMPS) and Total Access Cellular System (TACS). Second generation systems offer digital voice and low to medium-rate data communications (e.g. 9.6 kb/s). The main systems are Global System for Mobile Communications (GSM), Digital AMPS (DAMPS)/IS-136, Personal Digital Cellular (PDC), and cdmaOne/IS-95B. Third generation systems offer multimedia capabilities to second-generation platforms like support for high bit rates (144 kb/s to 2 Mb/s) and extended capabilities over second-generation systems [1-6].

CDMA-based systems are widely used in various wireless applications. In order to exploit the capacity of a CDMA system, employing multiuser detection techniques becomes essential. A large number of schemes and algorithms have been devised to enhance the performance and also to reduce the complexity of a CDMA receiver in a multiuser environment.

In most CDMA applications, some prior knowledge of the user parameters, e.g., the spreading code, timing of users, and power is assumed. However, in a real system, this may not be the case. Users enter and exit the system irregularly and the base station has to keep track of the status of each user. Various methods could be used to transfer users' parameters to the base station, however, one way or the other, they impose some overhead and reduce system capacity. Therefore, another important aspect of the CDMA

reception is to assist multiuser detection schemes by user identification and their parameters estimation.

In other words, it is desired to know how many active users are operating at any given time and who they are. This enables the receiver to dynamically adapt itself to a multiuser environment. This capability has a two-fold benefit for a CDMA multiuser system. First, the receiver will be able to maximize the cancellation of Multiple Access Interference (MAI), since it has the updated information on other active users. Second, the degree of complexity, which is almost directly proportional to the performance of the receiver, can be optimized against the number of active users. In other words, when there are a small number of users the receiver will be able to select a more complex detection algorithm to achieve a lower bit error rate. This is an attractive feature for software defined radio platforms.

Blind identification of users enables the receiver to be more self-reliant and it may also improve the system efficiency, since side information is not required. Currently, a great deal of complexity of a CDMA system is spent on establishing the basic synchronization that includes code or channel assignment tasks and so forth. Therefore a self-reliant scheme can notably reduce the task load of a base station. Moreover, a blind scheme that is capable of identifying users and their spreading sequences is very valuable for other applications such as: signal intercept, ad-hoc networking and non-intrusive performance evaluation tests.

## *1-2. Scope of the Work*

The most typical information needed in every CDMA network is the available random spreading codes and access slot in the cell. As the terminal cannot register to the cell without having access to the information, a broadcast channel is usually needed for transmission of such information. The broadcast channel is a transport channel that is used to transmit information specific for a given cell. This occurs with transmission of a relatively high power in order to reach all the users within the intended coverage area. Also, in an uplink CDMA, the base station does not have any control or knowledge of activity of users in adjacent cells. Therefore blind identification can assist the base station in estimation and cancellation of inter-cell interference. Thus, there is bandwidth as well as power penalty involved using a broadcast channel. This motivates the idea of user identification without reliance on any side information or a broadcast channel.

Acquiring information revealing the identity of an active user in a CDMA system without benefiting from a broadcast channel is called user identification. The type and extent of the information resulted from user identification process can be varied from one application to another. This information covers various parameter of an active user such as: spreading waveform, transmitted power, timing, direction of arrival. Many systems employ coordination between the transmitter and the receiver units to eliminate the necessity of acquisition of those parameters. For example, in order to initiate a call the mobile unit and the base station must follow certain protocols before being able to make a call. However such coordination causes extra cost and over-head on the system. Therefore it is desirable to minimize the reliance of a communication platform to any

supervisory information to improve the efficiency of the system. This opens the topic of blind identification of users that is the subject of this work.

## *1-3. Contribution of the Thesis*

Several user identification schemes have recently been introduced [18]-[27]. In all, the prior knowledge of the signature sequences or some other forms of constraint on the system are assumed, i.e., training sequences or direction of arrival of the signal. The main contribution of the thesis is that the proposed approach does not require the prior knowledge of the signature sequences nor it relies on other conditions or requirements called for in the previous works. The only parameters required to be available at the receiver are the processing gain and the rate of transmission that are basic parameters of the system.

In this work, a blind scheme based on Multiple Signal Classification (MUSIC) algorithm for user identification in a chip-synchronous multiuser CDMA system is suggested. The scheme is blind in the sense that it does not require prior knowledge of the spreading codes. Spreading codes and users' power are acquired by the scheme. Eigenvalue Decomposition (EVD) is performed on the received signal, and then all the valid possible signature sequences are projected onto the subspaces. However, as a result of this process, some false solutions are also produced and the ambiguity seems un-resolvable. Our approach is to apply a transformation derived from the results of the subspace decomposition on the received signal and then to inspect their statistics. Based on the difference in the statistics of a false and authentic solution, a cost function is defined. Then, the scheme searches over both signal subspace and time domain to

minimize the defined cost function. The proposed scheme is able to perform user identification without any external assistance in both symbol-synchronous and symbol-asynchronous CDMA systems.

## *1-4. Organization of the Thesis*

The thesis is organized in five chapters. In Chapter 2, a short overview of the CDMA system and basic definitions are presented. Also, a quick scan of the multiuser detection schemes is provided to highlight the requirement and importance of the prior information about users' parameters. Then, the topic of user identification and its applications in CDMA systems are presented. Finally, a summary of the prior works on the subject of user identification ends Chapter 2.

In Chapter 3, the proposed approach for blind identification of users is presented. The scheme relies on subspace decomposition of the received signal into orthogonal subspaces of signal and noise. System model is discussed and the proposed scheme for distinguishing between false and authentic solutions is introduced. Then, the method is analyzed for a synchronous system and then extended to an asynchronous case. Also, simulation results are presented to reflect the performance of the scheme.

Chapter 4 is dedicated to performance evaluation of the proposed method. The first subject discussed is how the algorithm can be accelerated in order to meet the speed required for a dynamic CDMA system where users can enter and exit the system at any time. The other topic discussed in the chapter is the performance evaluation of the scheme. The main measure of the performance is the probability of false and miss

detections. Thus, the false and miss probabilities are evaluated and analytical versus simulation results are compared.

In Chapter 5, concluding remarks are presented and the contributions of the thesis are highlighted. Furthermore, some suggestions for future work are presented. The suggestions are grouped into two groups. The first group covers suggestions for continuation of the work for the same application only with more stringent constraints. In the second group, possible extension of the proposed method to other applications is discussed.

# *Chapter 2*

## *User Identification in Multiuser CDMA Systems*

### *2-1. Introduction*

Ever increasing demands for wireless communication call for higher data rates, bandwidth efficient modulations as well as more efficient multiple access techniques. Multiple-access is one of the critical functions of any network. The two traditional multiple-access techniques, based on frequency and time division, are being employed in several applications for the past decades. CDMA has taken on a significant role in cellular and personal communications. CDMA has also gained interest for satellite applications, providing multimedia services over a larger number of audiences. To enhance the efficiency of CDMA, multiuser detection concept is introduced. As it will be explained in more detail in the next sections, multiuser detection enables each receiver to

detect the desired signal in presence of severe co-channel interference, resulting in a larger capacity for the whole network.

Although there are several flavors of CDMA-based spread spectrum system, such as: Frequency Hopping (FH) and Hybrid FH-DS, the focus of this work is only on DS-CDMA systems. Also, although the entire discussion holds for both base station and handset applications, the main focus of this work is more oriented for base station applications.

## *2-2. A Short Review of the CDMA History*

CDMA was first tried in the military field and for navigation systems [1]-[5]. In 1950, De Rosa-Rogoff proposed a Direct Sequence Spread Spectrum (DS-SS) system and introduced the concept of processing gain. In 1956, Rake concept was proposed by Price-Green. Between 1961 and 1978, cellular applications based on spread spectrum system were suggested. In 1980, DS-CDMA was proposed by Qualcomm and later they would offer $2^{nd}$ generation CDMA radio network. In July 1993, IS-95 standard and narrow band CDMA were introduced. Commercial applications of IS-95 and multiuser detection and MLSE (maximum likelihood sequence estimation) concept in AWGN channel were formulated in 1996 by Verdu. During the 1990s, wideband CDMA techniques with a bandwidth of 5 MHz or more have been investigated and several standards such as FRAMES-FMA2 in Europe, Core-A in Japan and CDMA2000 in the United States [6] are introduced. These standards that constitute the third-generation of wireless mobile communication systems, or so-called 3G, are expected to be widely

deployed by 2010. Meanwhile, forth generation system definition and development have already begun.

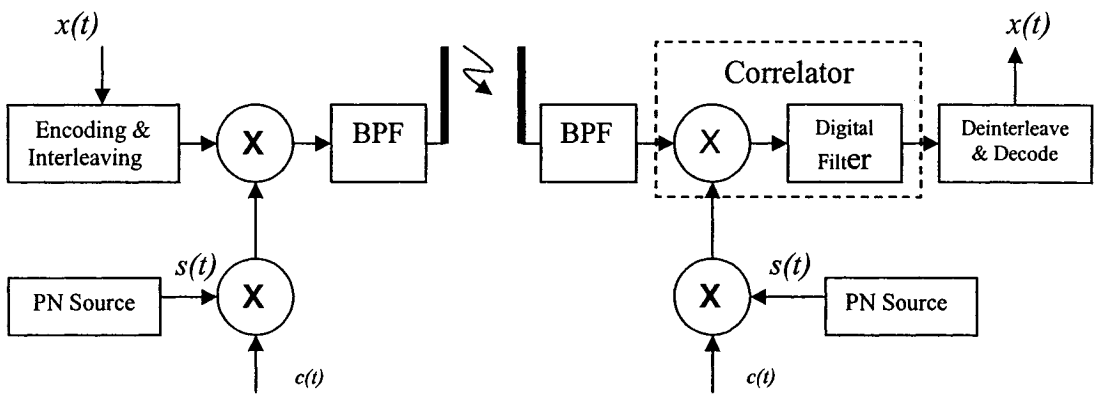


**Figure 2.1 A Basic BPSK DS-CDMA system**

## *2-3. DS-CDMA Principle*

In CDMA, as the name implies, each user is assigned a distinct code to encode its information bearing signal. Figure 2.1 shows a simple implementation of a BPSK DS-CDMA system. The data stream, *x(t)*, is processed by the encoder block and enters the modulator with a rate of $R_b$ bit/s. It is modulated by the carrier *c(t)* and the spreading code *s(t)*. The spreading or signature sequence *s(t)* is generated at a rate of $R_c$ chips/s by the Pseudo-Noise (PN) generator block. This block produces a deterministic sequence, which has a very long period replicating a real random sequence. The rate at which the spreading sequence is generated is called the chip rate. Chip rate is usually much higher than the data rate $R_b$. The ratio

$$N = \frac{R_c}{R_b} \tag{2.1}$$

defines the processing gain of the system. Following the encoding process, the bandwidth of the spreading code is much larger than the bandwidth of the information bearing signal. Processing gain determines the amount of spreading of the original signal.

At the receiver, we assume an established synchronization at carrier, clock and code levels. The received signal, after the down-conversion, is correlated with the local signature signal. If the signature sequence of that receiver is the same as the one used in the transmitter, the correlator de-spreads the received signal successfully. That can be accomplised since the correlation between the desired user's code and other users' code is assumed to be negligible. The de-spread signal is decoded and processed to regenerate *x(t)*. However, as Figure 2.2 shows, if the codes are different, the correlator spreads the signal even further and protects the privacy of the link.

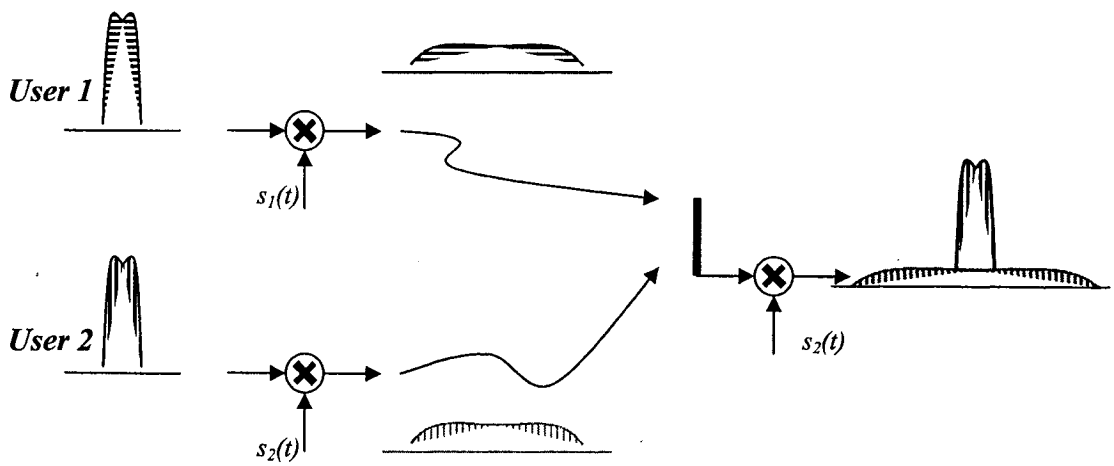


**Figure 2.2 De-spreading the received signal at the receiver**

## *2-3.1. CDMA Features*

In general there are certain features of the DS-CDMA that make it very attractive for various applications [1]-[6]:

*Multiple access*: By spreading, the original signal is virtually buried in background noise both in time and frequency domain. This not only gives discreteness and Low-Probability of Intercept (LPI), but also offers the opportunity of overlaying low level DS-CDMA on top of existing narrow-band users and improving the network capacity.

*Interference rejection*: The interference could be a hostile interference, like a jammer, or a simple case of simultanous use of the channel by other users in the system. In either case, the de-spreading operation at the receiver improves the signal to interference ratio by the processing gain $N$. In the case of a narrow-band interferer, at the receiver, the interference signal is correlateded by the spreading code resulting in spread of the narrow-band interferer over a larger frequency and reduction of its power spectral density.

*Robust multipath performance*: Since the ideal autocorrelation of a spreading code vector is zero outside the code interval, the multipath signals will be threated as an interfering signal and hence, its influence on the information-bearing signal will be limited.

*Soft capacity*: As mentioned earlier, CDMA has a soft capacity. This means that the capacity of the system can be enhanced to some extent by simply tolerating some degradation on the Bit Error Rate (BER) performance of the system.

*Security*: This can be interpreted in two ways, privacy and low probability of interception. In the case of privacy, the transmitted data can be recovered if and only if the code used to transmit the data is known at the receiver. Hence, any attempt for eavesdroping fails, if the assigned spreading code for the chanel is not a priori known. On the other hand, the first step for a hostile interferer or eavesdropper is to locate the used

channel. Since the spread data has a very low power spectral density, it is quite difficult to detect the spread spectrum signal across the whole frequency band. This provides a satisfactory level of LPI for many applications.

## 2-3.2. CDMA Limitations

There are two main problems associated with a CDMA system [7]-[8]:

*Multiple Access Interference (MAI):* In a conventional DS-CDMA system, each user processes its own signal and treats the other users' signals as additive noise. In this approach, the only protection for combating MAI is provided by inherent suppression capability of CDMA, measured by the processing gain *N*. This interference suppression capability is, however, limited and as the number of users grows, some degradation is introduced in BER performance of the system. This problem arises from the fact that the spreading codes of different users are not orthogonal, and hence in the de-spreading of a given user's signal, there will be some contribution from other users' signals.

*Near-far problem:* The near-far problem arises when the signals from different users arrive at the receiver with widely varying power levels. In the case of a large difference, a strong user could overwhelm all the weaker signals. This problem could be a serious limiting factor for the capacity of a system, unless is taken care of by using a power control algorithm. The difference in the power between different users can be originated from either having different physical distances to the base station or experiencing a deep fade during the signal reception.

## 2-3.3. *CDMA Receiver Model*

Figure 2.3 shows a DS-CDMA system with K users. They all operate at the same data rate of $R_b$, sharing the same allocated channel. A synchronous DS-CDMA system is considered with a processing gain of $N$. The received signal prior to chip rate sampling can be modeled as

$$r(t)=\sum_{k=1}^{K} A_k b_k s_k(t)+n(t) \quad t\in(0,T] \tag{2.2}$$

where $A_k$, $b_k$ and $s_k(t)$ denote the received amplitude, transmitted bit and the spreading sequence of the $k_{th}$ user, respectively. $A_k$ is assumed to be unknown but constant during the period of observation. $b_k$ is a random variable taking values $\pm 1$ with equal probability. Spreading codes are assumed short, i.e., supporting only the bit interval $T$. The white Gaussian noise with a variance of $\sigma^2$ is denoted as $n(t)$.

After the chip rate sampling, Equation (2.2) can be written in a vector form as

$$\mathbf{r}=\sum_{k=1}^{K} A_k b_k \mathbf{s}_k + \mathbf{n} \tag{2.3}$$

where $\mathbf{s}_k=\left(1/\sqrt{N}\right)\left[s_{k1}\ s_{k2}\cdots s_{kN}\right]^T$ represents the normalized signature sequence of the $k_{th}$ user. Superscript $^T$ denotes the transpose operation, $\mathbf{n}$ is a zero mean white Gaussian noise vector with a covariance matrix $\sigma^2\mathbf{I}_N$, where $\mathbf{I}_N$ is the $N \times N$ identity matrix. For convenience Equation (2.3) can be rewritten as

$$\mathbf{r}=\mathbf{SAb}+\mathbf{n} \tag{2.4}$$

where $\mathbf{S}=[\mathbf{s}_1\ \mathbf{s}_2\cdots\mathbf{s}_K]$, $\mathbf{A}=\mathrm{diag}\left[A_1\ A_2\cdots A_K\right]$ and $\mathbf{b}=[b_1\ b_2\cdots b_K]^T$.

At the receiver, the detector is responsible for separating users' signals and detecting their corresponding information bits. In Figure 2.3, the $i_{th}$ estimated information bit is represented by $b_i'$.

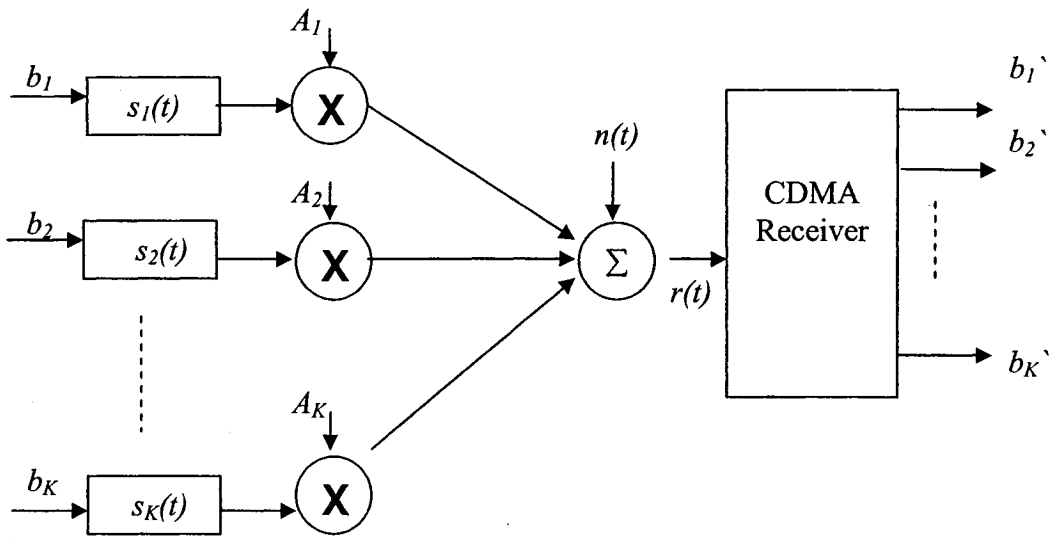


**Figure 2. 3 A simple presentation of a CDMA channel**

## 2-3.4. *Conventional CDMA Receiver*

A conventional receiver consists of a bank of correlators, each matched to a corresponding spreading code [5]. The detectors outputs are sampled at each bit interval and the decision is made based on the sign of the samples. This can be shown as

$$\begin{aligned} \mathbf{y} &= \mathbf{S}^T\mathbf{r} = \mathbf{S}^T\mathbf{S}\mathbf{A}\mathbf{b} + \mathbf{S}^T\mathbf{n} \\ &= \mathbf{R}\mathbf{A}\mathbf{b} + \mathbf{S}^T\mathbf{n} \end{aligned} \tag{2.5}$$

where $\mathbf{R} = \mathbf{S}^T\mathbf{S}$ is the cross-correlation matrix of the spreading waveforms. In practice, the spreading waveforms are not orthogonal, therefore $\mathbf{R}$ will not be a diagonal matrix.

Hence, there will always be some interference from other users. A conventional CDMA receiver treats MAI as AWGN; therefore it has a limited performance in a multiuser environment. As cited earlier, the performance of the conventional detector vastly depends on the number of active users in the system and their relative powers.

## *2-4. Multiuser Detection for CDMA Systems*

As stated earlier, a conventional CDMA receiver has two main drawbacks, i.e., MAI and near/far problem. They both originate from the interference of other users and cause a degradation of performance. To overcome the shortcomings of a conventional CDMA system, transmit-oriented techniques and receive-oriented techniques are introduced. Power control algorithms and spreading with orthogonal codes belong to the former and multiuser detection [8]-[9] is the core subject of the latter. Potential capacity increase and near/far resistance can be achieved if the negative effect that each user has on others can be cancelled. Hence, using joint detection of users, the destructive effect of MAI can be significantly reduced. Although the idea is easy to comprehend, the implementation could be very complex [8]-[10]. Here a short review of some of the principle multiuser schemes is presented.

### *2-4.1. The Optimum Detector*

The optimal detection is based on the Maximum Likelihood Sequence Estimation (MLSE) [11]. The objective is to find the sequence, which maximizes the conditional likelihood of the given sequence. The maximum likelihood decision for the vector $\mathbf{b}'$ is given by:

$$\arg\left\{\max_{\mathbf{b}\in\{-1,+1\}^K}\left[2\mathbf{y}^T\mathbf{A}\mathbf{b}`-\mathbf{b}`^T\mathbf{A}\mathbf{R}\mathbf{A}\mathbf{b}`\right]\right\}. \tag{2.6}$$

The estimated elements of the input vector are evaluated based on a search over all $2^K$ possible combinations of the original input vector $\mathbf{b}`$. This can be implemented using the Viterbi algorithm. The optimum detection shows an excellent performance approaching single user bound, also it is capable of overcoming the near/far problem. As Equation (2.6) shows, the scheme requires the knowledge of amplitudes of all users. From the practical point of view, this technique is prohibitively complex to be implemented; it has $2^{K-1}$ states and requires $K$ storage updates per symbol interval. The complexity grows exponentially and this is a major drawback of this method.

## *2-4.2. The Linear Decorrelating Detector*

Multiplying the two sides of the Equation (2.5) by $\mathbf{R}^{-1}$, the inverse of the cross-correlation matrix, leads to the linear decorrelating detection scheme [8], [12]. The resulting vector is:

$$\mathbf{R}^{-1}\mathbf{y} = \mathbf{A}\mathbf{b} + \mathbf{R}^{-1}\mathbf{n} \tag{2.7}$$

resulting in the information vector $\mathbf{b}$ plus a new noise term. Since the new noise term still has zero mean, the decision will be based on:

$$\mathbf{b}` = \mathrm{sgn}\left(\left[\mathbf{R}^{-1}\mathbf{y}\right]_K\right) = \mathrm{sgn}\left(\left[\mathbf{A}\mathbf{b} + \mathbf{R}^{-1}\mathbf{n}\right]_K\right). \tag{2.8}$$

A very important feature of the decorrelator detector is that, unlike the optimum detector, it does not need the prior knowledge of the signal powers. Equation (2.8) shows that neither signal nor noise terms are influenced by the interference. Hence the

performance will be independent of the strength of the interfering users, and the decorrelator receiver is capable of combating the near/far problem. Decorrelator receiver is less complex than the optimum detector and its complexity grows linearly with the number of users. One of the issues regarding the use of the decorrelator detector is that the cross correlation matrix of the spreading code has to be known a-priori or estimated for each detection interval. Also, since a decorrelator detector does not take into consideration the noise term, the decorrelation process leads to noise enhancement.

## *2-4.3. The Minimum Mean-Square Error Detector*

To address the drawback of the decorrelator, Minimum Mean-Square Error (MMSE) detector is devised [12]-[13]. MMSE detector is a linear receiver that minimizes the mean square error:

$$\min_{\mathbf{M}\in R^{K\times K}} E\left[\left\|\mathbf{b}-\mathbf{My}\right\|^2\right] \tag{2.9}$$

where **M** is found as the optimal solution:

$$\mathbf{M}=\left[\mathbf{R}+\sigma^2\mathbf{A}^{-2}\right]^{-1}. \tag{2.10}$$

It provides a considerable level of MAI rejection while maintaining additive noise term at a very low level. The receiver structure for this method is very similar to the decorrelating detector. The only difference is replacing the processor block $\mathbf{R}^{-1}$ by $\mathbf{M}=\left[\mathbf{R}+\sigma^2\mathbf{A}^{-2}\right]^{-1}$. The conventional matched filter receiver is basically optimized to fight the background white noise exclusively, whereas the decorrelating detector eliminates the multiuser interference disregarding the background noise. In contrast, the

MMSE linear detector can be seen as a compromise solution that takes into account the relative importance of each interfering user and the background noise. In fact both the conventional receiver and the decorrelating receiver are limiting cases of the MMSE linear detector. For this type of receivers, the prior knowledge of users' power is required. The complexity of the receiver grows linearly with the number of users, and the required computation involves matrix inversion.

## *2-4.4. The Decorrelating Decision Feedback Detector*

The decision feedback detectors [8], [14] are characterized by two matrix transformations: a forward filter and a feedback filter. These detectors are similar to decision feedback equalizer used to fight inter-symbol interference for single user applications. However, in addition to equalization, the decision feedback multiuser detectors employ successive cancellation. In each time frame, decisions are made in the order of decreasing users' strengths. The receiver makes the decision for stronger users first, allowing weaker users benefiting from this information toward their own decisions. The receiver structure can be motivated from the following. The cross-correlation matrix $\mathbf{R}$ can be factorized by Cholesky method as:

$$\mathbf{R} = \mathbf{F}^T\mathbf{F} \tag{2.11}$$

where F is a lower triangular matrix. The output vector of the matched filter bank after multiplying by $\left[\mathbf{F}^T\right]^{-1}$ is:

$$\bar{\mathbf{y}} = \mathbf{FAb} + \bar{\mathbf{n}} \tag{2.12}$$

where $\bar{\mathbf{n}}$ is a Gaussian vector. The output vector after cancellations becomes:

$$\mathbf{b}` = \mathrm{sgn}\left(\mathbf{F}^{-T}\mathbf{y} - \left(\mathbf{F} - diag[\mathbf{F}]\right)\mathbf{A}\mathbf{b}`\right). \quad (2.13)$$

Best performance is achieved when at the receiver a power sorter precedes Cholesky factorization. So that the strongest is ranked first, and the weakest is ranked last. As such, the signal of the strongest user, that is least corrupted by MAI, is detected first. This decision is then used to subtract MAI from the signal of the second user, and so forth.

The performance of the decorrelating decision feedback detector for weak users is superior to the conventional and the linear decorrelating detector. This detection method requires the knowledge of users' signal strength. In terms of the complexity, it requires to perform Cholesky factorization and matrix inversion.

## 2-4.5. *The Successive Interference Canceller*

The successive interference cancellation [15] is motivated by the idea of a simple augmentation of the conventional detector in order to achieve multiuser detection. The output after $k_{th}$ cancellation equals to:

$$y(t) - \sum_{j=1}^{k-1} a_j b_j R_{kj} \quad (2.14)$$

and the bit decision for the $k_{th}$ user is:

$$b_k` = \mathrm{sgn}\left[ y(t) - \sum_{j=1}^{k-1} a_j b_j R_{kj} \right]. \quad (2.15)$$

where $R_{kj}$ is the $kj_{th}$ element of the **R**. To remove the MAI, the knowledge of users' amplitude and also their decisions are required. These can be obtained by separate estimation of each or directly by using the output of a decorrelator. Similar to the

decision feedback detector, it is important to cancel the strongest signal before detection of the other signals. The benefit of cancellation in order of signal strength is twofold. First, canceling the strongest signal has the most benefit because it has the most negative effect. Secondly, canceling the strongest signal is the most reliable cancellation and also provides the best bit decision.

In this technique, there is one bit delay per stage of cancellation. Therefore the number of cancellation has to be traded off with the complexity and the maximum delay requirement of the receiver.

## *2-4.6. The Multistage Interference Cancellation*

The multistage interference canceller in principle is similar to the two above detection schemes [16]-[17]. The term multistage detection is suggested by the fact that various decisions are produced at consecutive stages. The $i_{th}$ stage of this detector uses decisions of the $(i\text{-}1)_{st}$ stage to cancel MAI present in the received signal. The decision for the $i_{th}$ stage of cancellation is:

$$b'^{\,i}_{k} = \mathrm{sgn}\left[y_k - I_k^{(i-1)}\right] \tag{2.16}$$

where $I_k^{(i-1)}$ is the estimated interference for $k_{th}$ user in the $(i\text{-}1)_{st}$ stage of cancellation,

$$I_k^{(i-1)} = \sum_{j \neq k} a_j b'^{\,(i-1)}_{k} R_{kj} \,. \tag{2.17}$$

The performance of multistage detector depends on the relative energies of the users. It best performs for equal power users.

## 2-4.7. *Summary of the schemes*

Table 2.1 shows a comparison between various main multiuser detection schemes. As presented, in every scheme, some advance information on users are required for successful detection.

| *Scheme* | *Principle* | *Features* | *Disadvantages* |
|---|---|---|---|
| ***Conventional Receiver*** | Correlators bank | • Minimum cost and complexity | • Not near-far resistant<br>• Severe degradation due to MAI |
| ***Optimum Detector*** | Maximum Likelihood Sequence Estimation (MLSE) employing Viterbi algorithm | • Outstanding performance in MAI cancellation | • Very complex implementation<br>• Prior knowledge of all users' powers |
| ***Linear Decorrelating Detector*** | Decorrelating the received signals by multiplying the received vector by the inverse of the cross-correlation matrix | • Complete cancellation of MAI<br>• No need for prior knowledge of all users power | • Noise enhancement<br>• Prior knowledge or real-time estimation of matrix $\mathbf{R}^{-1}$ |
| ***Minimum Mean-Square Error (MMSE) Detector*** | Minimizing the mean square error of: $\min_{\mathbf{M}\in R^{K\times K}} E\left[\left\|\mathbf{x}-\mathbf{My}\right\|^2\right]$ | • Relatively good performance | • Prior knowledge of users' powers<br>• Requires matrix inversion |
| ***Decorrelatig Decision Feedback Detector*** | Cholesky factorization of $\mathbf{H}$ | • Better performance than MMSE. | • Power sorting<br>• Requires Cholesky factorization as well as matrix inversion<br>• Prior knowledge of all users' powers |
| ***Successive Interference Canceller*** | Canceling interference starting form the strongest to the weakest. | • Near-far resistance. | • Power sorting<br>• One bit delay per cancellation stage<br>• Prior knowledge of all users' powers |

**Table 2.1 – A summary of main multiuser detection schemes**

## 2-5. *User Identification in CDMA Systems*

Acquiring information revealing identity of an active user in a CDMA system is called user identification. The type and extent of the information resulted from user identification process can vary from one application to another. This information covers various parameter of an active user such as: spreading waveform, received power, timing, direction of arrival and so on [18]-[29]. Many systems employ coordination between the transmitter and the receiver units to eliminate the necessity of the acquisition of those parameters. For example, in order to initiate a call the mobile unit must send and receive certain signals to and from the base station before being able to make a call. However, such coordination causes extra cost and over-head on the system. Therefore, it is desirable to minimize the reliance of a communication platform on any supervisory information to improve the efficiency of the system. This is the topic of blind identification of users that is the subject of this thesis.

### 2-5.1. *User Identification in Multiuser Detection*

In a DS-SS system, users operate in the allocated channel simultaneously. Since the spreading waveforms are not always orthogonal, there is interference between the users. Multiuser detection schemes are developed to combat the Multiple Access Interference (MAI). The promise of performance enhancement by multiuser detection is valid provided availability of information about each user, such as: spreading waveforms, users' relative delays and users' powers. The parameters needed to characterize a multiuser environment are dynamic. The dynamism originates from the mobility of users, and burstiness of the transmission. Therefore, it is essential to maintain updated

information about users. Unless those parameters become available through some coordination, i.e., by employing a side channel, they must be estimated and tracked. Using a side channel to supply such information requires extra bandwidth and imposes extra cost and complexity.

Even if some form of coordination exists between the mobile and the base station, this information may be available only within a cell. Therefore, these parameters cannot be accessed, if the interference is originated from the adjacent cells. Also, if users are not symbol synchronous, the a-priori knowledge of the spreading waveforms is not conclusive, since users' timings are still to be found. Therefore, an efficient multiuser detection scheme requires performing user identification as well.

### *2-5.1.1. Case Study; Decorrelator Multiuser Detector*

In this subsection, through an example, the importance of user identification for decorrelator receiver is shown. Figure 2.4 shows a basic structure of the receiver comprising of a correlator bank and the decorrelator function itself.

Figure 2.4 shows the Bit Error Rate (BER) performance of a multiuser system with and without user identification. The processing gain $N$=16, and all users are assumed equal power with a signal-to-noise ratio of 12dB. The matched filter receiver or traditional CDMA receiver that does not employ a multiuser approach exhibits worst performance. In such scenario, the BER of the system degrades quickly as the number of active users increases. However by using a decorrelator detector in conjunction with the matched filter, the BER performance improves as demonstrated in Figure 2.4.

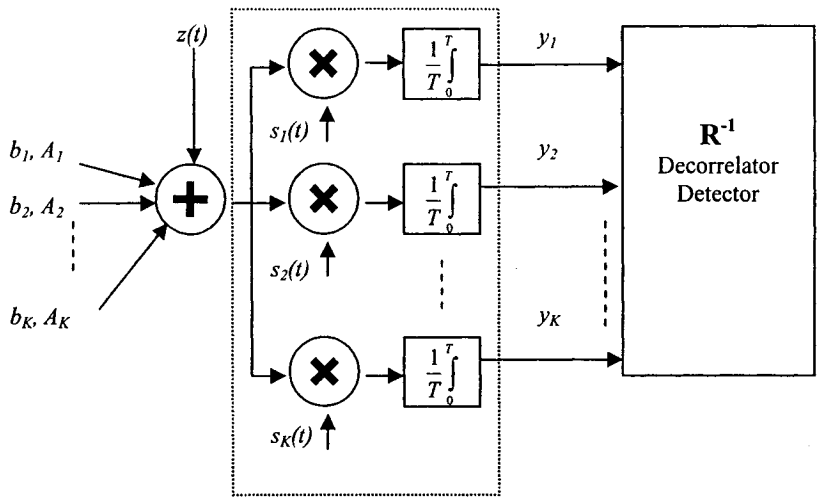


**Figure 2.4 A decorrelator receiver**

This improvement is possible if the receiver knows exactly who the active users are and then comes up with the appropriate decorrelating transform. If that information is not available, the performance will deteriorate and it might even become worse than a receiver that does not have any multiuser detection. For example, if the number of users drops and the receiver does not acquire this information and still continues to employ the un-updated decorrelation, the performance is degraded. This is shown by the curve using the third legend. In this case, the receiver assumes that there are 14 active users in the system and applies that information for any number of users. As Figure 2.5 shows, in such a scenario, for small number of users the performance is even significantly worse than a single user receiver.

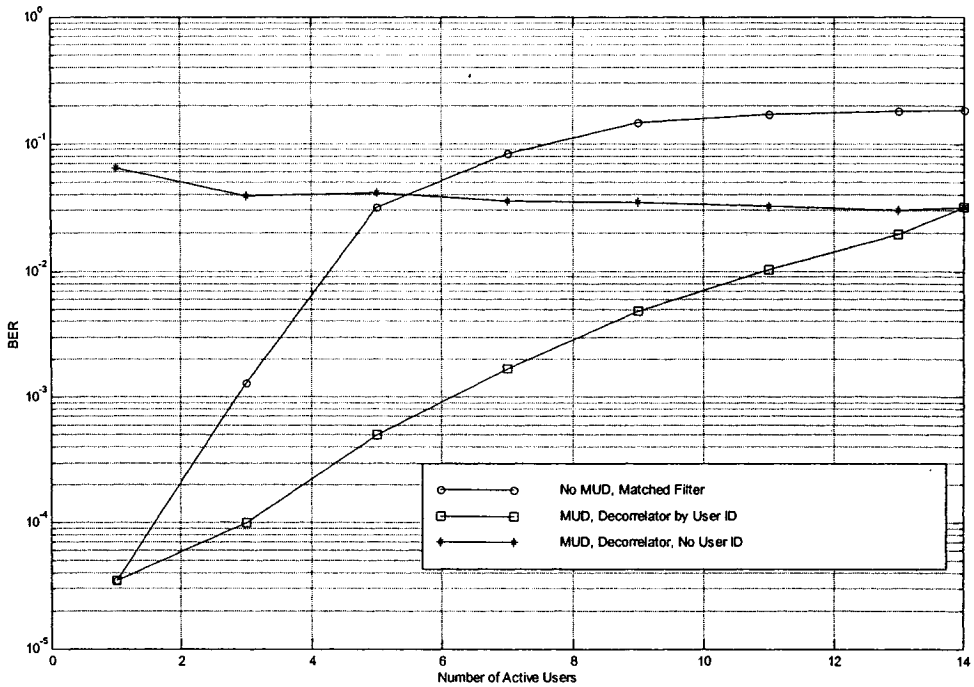


**Figure 2.5 BER performance with and without user identification**

## *2-5.2. Eavesdropping and Signal Intercept*

Military and law-enforcement agencies employ SS-based systems extensively. While SS techniques propose basic steps towards security of a friendly link, they make it more difficult to intercept a hostile transmission using such system. For eavesdropping and signal intercept applications, we have to add new dimensions to the dynamism of a multiuser environment; the dimensions are spreading waveforms and relative delays of the targeted users. In a hostile or non-cooperative scenario, users may not employ any predefined spreading waveforms and may often change their spreading codes. Therefore, the first step for signal interception is to determine spreading waveforms and relative

delays of the operating users. From there, all other parameters of the user can be estimated and the targeted signal could be successfully detected.

## 2-5.3. *Ad-Hoc Networking*

In an Ad-Hoc wireless network with $M$ nodes, $O(M^2)$ orthogonal channels are required. For efficient implementation of such networks, the allocated bandwidth should be optimized. This means that for a CDMA based Ad-Hoc network, $N<<M^2$ [18]. This can be achieved if a user, just before setting-up a connection, assesses the traffic of the channel by identifying the identity of each active user and the usage of spreading codes. Then, from the pool of the remaining available codes, one waveform can be selected and be used for the call. The selection can be even done based on the amount of the cross-correlation that it could have with the other used spreading codes. Thus in order to minimize interference, the one that results minimum cross-correlation will be selected.

## 2-5.4. *Non-intrusive Performance Evaluation*

In many applications, such as cellular wireless system, existing test procedures require that the test equipment simulate the functionality of one hop in order to test the performance of the other hop. However, a wireless communication platform can be tested and its performance be evaluated by monitoring the transactions between the two working hops. This technique avoids cutting off the link and disrupting the flow of information.

To implement such technique in a DS-CDMA based system, it is essential that the monitoring equipment be able to acquire all the required information simply by listening

to the signal in the air. This is another application of blind estimation of spreading waveform and user parameters.

## 2-6. *Prior Works*

Several schemes for user identification in a DS-CDMA system have been introduced. They can be sorted based on the amount of expected information about each user available to the receiver and also the presumed conditions. Here, we review main schemes that are most cited in literatures.

In [19], Chang et al propose an approach for user identification and parameter estimation in an AWGN channel. In their proposed scheme, a filter bank with each branch matched to a given signature sequence is used. The outputs of the matched filters are further processed to identify the activity of users. The scheme requires the advance knowledge of spreading waveforms. Also it is inefficient, since it always has to process the receive signal as if all the users are active.

Yu et al presented a technique for user identification without relying on users' spreading waveforms that employs an antenna array [20]. The approach is limited to cases when users' signals arrive at the receiver from different angles. Therefore in a practical scenario, where users are located randomly, the proposed scheme fails to identify the users who are in a same proximity.

The approach proposed by Halford et al [21] relies on two important requirements. It needs to know the spreading waveforms of all users in advance and also the identity of the current active users in order to identify a new active user.

Schemes based on the subspace theory have been proposed for blind channel estimation as well as blind detection for a CDMA multiuser receiver [28]-[30]. The subspace concept has also been used for user identification in a CDMA system [22]-[25]. Techniques presented in [22]-[23] and [25], all require advance knowledge of the spreading waveforms. Zhang et al proposed a technique for blind estimation of signature waveforms, yet it relies on training sequences sent by the transmitter.

The paper by Wu et al [25] presented a subspace approach based on Multiple Signal Classification (MUSIC) algorithm for a synchronous DS-CDMA. This scheme also requires the prior knowledge of all the signature sequences. In this work, it is assumed that the system is a symbol-synchronous CDMA system with all the spreading waveforms available in a pool. Then, by having access to this pool, the active users are detected by inspecting their signal subspace properties. The work by Wu has stemmed several other studies on the subject [18], [26]-[27], yet they all share the same restriction of requiring prior knowledge of the spreading waveforms. Moreover, the work presented in [27] requires frequent transmission of training signals.

In this thesis, we propose an approach for blind identification of active users in a DS-CDMA system. It can be employed for both synchronous and asynchronous models. The

approach does not rely upon any training signal and does not require any prior knowledge about the activity, spreading waveforms, power or relative delays of users. Basically, this work addresses the shortcomings of previous works, namely, requiring advance knowledge of the signature waveforms, assumption of a symbol-synchronous channel, necessity of training epochs and presumption of different direction of arrival for each user.

# *Chapter 3*

## *Blind Estimation of Spreading Waveforms and Users' Timings*

### *3-1. Introduction*

A blind scheme is proposed for blind discovery of spreading waveforms and timing estimation in a DS-CDMA system. The model throughout this work is based on a chip-synchronous DS-CDMA with symbol-asynchronous users. Hereafter, synchronous or asynchronous refer only to the timing of the active users.

The approach does not require any advance knowledge of users' parameters or any training signal. The scheme is based on the subspace decomposition and searches for solutions that minimize a defined cost function. Minimizing the cost function leads to the elimination of false solutions that originate from linear combination of active users and

also acquiring the timing of the active users. The search is performed over both waveform and time domains.

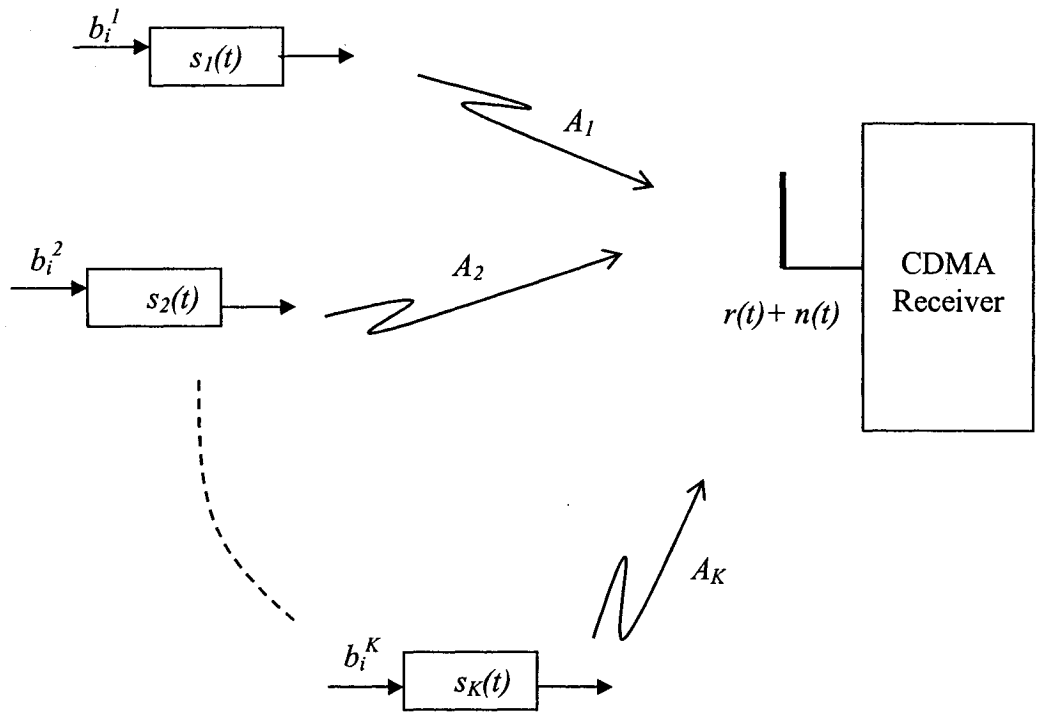


**Figure 3.1 A basic graph of the system for user identification**

## *3-2. Problem Formulation and Signal Model*

Figure 3.1 shows a chip-synchronous BPSK DS-CDMA system with $K$ active users. Equation (3.1) is a mathematical presentation of such system operating over a Rayleigh fading channel. The spreading factor is assumed to be $N$. The received baseband signal prior to chip rate sampling can be expressed as

$$r(t)=\sum_{k=1}^{K} A_k b_k s_k(t-\tau_k)e^{j\theta_k}+n(t) \quad t\in[0,T] \tag{3.1}$$

where $b_k$ and $s_k(t)$ denote the transmitted bit and the spreading sequence of the $k_{th}$ user, respectively. During transmission, each user's signal can be subjected to uncorrelated Rayleigh fading. This is implemented in Equation (3.1) by $A_k$ where

$$A_k = |A_k| e^{j\phi_k} \tag{3.2}$$

where $|A_k|$, is the $k_{th}$ active user's Rayleigh distributed amplitude with second order moment $E\left(|A_k|^2\right) = \gamma_k{}^2$. The channel random phase shift $\varphi_k$ is uniformly distributed over $[0, 2\pi)$. We assume that the channel is a slow fading channel, i.e., channel parameters are constant during at least one symbol interval. $b_k$ is an euiprobable random variable taking ±1. Spreading codes are assumed short; supporting only the bit interval $T$. The white complex Gaussian noise with a variance of $\sigma^2$ is denoted as $n(t)$. The delay of each user is represented by $\tau_k \in [0, T)$ and is equal to a multiple of the chip period $T_c$, i.e., $\tau_k = m_k T_c$ where $m_k$ is a positive integer smaller than $N$. The residual random carrier phase corresponding to each user is shown by $\theta_k$ that is uniformly distributed over [0, 2π).

Hereafter, we only consider an AWGN channel and also assume that users' amplitudes are constant during the observation intervals. After chip rate sampling, for the $i_{th}$ bit interval, Equation (3.1) can be written in a vector form as

$$\mathbf{r}(i) = \sum_{k=1}^{K} A_k e^{j\theta_k} \left\{ b_k^{i-1} \mathbf{D}_{m_k}^{p} + b_k^{i} \mathbf{D}_{m_k}^{c} \right\} \mathbf{s}_k + \mathbf{n} \tag{3.3}$$

where $\mathbf{s}_k = \left(1/\sqrt{N}\right)\left[s_{k1}\ s_{k2} \cdots s_{kN}\right]^T$ represents the normalized signature sequence of the $k_{th}$ user [31]. Noise is represented in a vector form as $\mathbf{n}$ with a covariance matrix $\sigma^2 \mathbf{I}_N$, where $\mathbf{I}_N$ is the $N \times N$ identity matrix. $\mathbf{D}_{m_k}^{p}$ and $\mathbf{D}_{m_k}^{c}$ are permutation matrices that are defined based on the delay of the $k_{th}$ user. The two matrices determine the contribution of

the previous and current bits within the collection window. They can be expressed in block forms as

$$\mathbf{D}_{m_k}^{p} = \begin{bmatrix} \mathbf{0} & \mathbf{I}_{m_k \times m_k} \\ \mathbf{0} & \mathbf{0} \end{bmatrix}_{N \times N} \tag{3.4}$$

$$\mathbf{D}_{m_k}^{c} = \begin{bmatrix} \mathbf{0} & \mathbf{0} \\ \mathbf{I}_{N-m_k \times N-m_k} & \mathbf{0} \end{bmatrix}_{N \times N}. \tag{3.5}$$

For convenience Equation (3.2) can be rewritten as

$$\mathbf{r}(i) = \mathbf{S}\mathbf{A}\boldsymbol{\theta}\,\mathbf{b}(i) + \mathbf{n} \tag{3.6}$$

where

$$\mathbf{S} = \left[\mathbf{D}_{m_1}^{p}\mathbf{s}_1 \quad \mathbf{D}_{m_1}^{c}\mathbf{s}_1 \cdots \mathbf{D}_{m_K}^{p}\mathbf{s}_K \quad \mathbf{D}_{m_K}^{c}\mathbf{s}_K\right]_{N \times 2K} \tag{3.7}$$

$$\mathbf{A} = \operatorname{diag}\left[A_1 \; A_1 \; \cdots A_K \; A_K\right]_{2K \times 2K} \tag{3.8}$$

$$\boldsymbol{\theta} = \operatorname{diag}\left[e^{j\theta_1} \; e^{j\theta_1} \; \cdots e^{j\theta_K} \; e^{j\theta_K}\right]_{2K \times 2K} \tag{3.9}$$

$$\mathbf{b}(i) = \left[b_1^{i-1} \; b_1^{i} \; \cdots b_K^{i-1} \; b_K^{i}\right]^{T}_{2K \times 1}. \tag{3.10}$$

Matrix **S** contains the effective signature waveforms that spread portions of the two consecutive bits of each user within the collection window. So that users do not cancel each other's signals, it is assumed that **S** has a rank of $2K$.

## *3-3. Signal and Noise Subspaces*

The autocorrelation matrix of the collected samples of the received signal can be evaluated as

$$\begin{aligned}\mathbf{C} &= E\left\{\mathbf{r}(i)\mathbf{r}(i)^H\right\} \\ &= \mathbf{S}E\left\{\mathbf{A}\boldsymbol{\theta}\mathbf{b}(i)\mathbf{b}(i)^T\boldsymbol{\theta}^H\mathbf{A}^H\right\}\mathbf{S}^T + \sigma^2\mathbf{I}_N \\ &= \mathbf{S}E\left\{\mathbf{A}\mathbf{A}^H\right\}\mathbf{S}^T + \sigma^2\mathbf{I}_N \\ &= \mathbf{S}\boldsymbol{\Gamma}\mathbf{S}^T + \sigma^2\mathbf{I}_N\end{aligned} \tag{3.11}$$

where

$$\boldsymbol{\Gamma} = \text{diag}\left[\gamma_1^2\ \gamma_1^2\ \gamma_2^2\ \gamma_2^2 \cdots \gamma_K^2\ \gamma_K^2\right]. \tag{3.12}$$

Since noise is assumed white and independent from the users' signals, then the received signal can be decomposed into orthogonal subspaces. Performing Eigenvalue Decomposition (EVD) on the autocorrelation matrix of the received signal results in two orthogonal subspaces of signal and noise [25].

$$\mathbf{C} = \mathbf{U}\boldsymbol{\Lambda}\mathbf{U}^T = \left[\mathbf{U}_s\ \mathbf{U}_n\right]\begin{bmatrix}\boldsymbol{\Lambda}_s & \mathbf{0} \\ \mathbf{0} & \boldsymbol{\Lambda}_n\end{bmatrix}\begin{bmatrix}\mathbf{U}_s^T \\ \mathbf{U}_n^T\end{bmatrix} \tag{3.13}$$

where $\mathbf{U}$ and $\boldsymbol{\Lambda}$ are the general eigenvector and eigenvalue matrices. Since the autocorrelation matrix $\mathbf{C}$ is symmetric, then all the eigenvalues are positive [34]. Matrices $\mathbf{U}_n$ and $\mathbf{U}_s$ represent eigenvectors of noise and signal subspaces, respectively. The signal and noise subspaces can be separated as follows:

- $\mathbf{U}_s$: The signal subspace

$$\boldsymbol{\Lambda}_s = \text{diag}\left[\lambda_1\ \lambda_2 \cdots \lambda_P\right] \tag{3.14}$$

$$\mathbf{U}_s = \left[\mathbf{u}_1\ \mathbf{u}_2 \cdots \mathbf{u}_P\right] \tag{3.15}$$

- $\mathbf{U}_n$: The noise subspace, for all $\lambda_i = \sigma^2$

$$\boldsymbol{\Lambda}_n = \text{diag}\left[\lambda_{P+1}\ \lambda_{P+2} \cdots \lambda_N\right] \tag{3.16}$$

$$\mathbf{U}_n = \left[\mathbf{u}_{P+1}\ \mathbf{u}_{P+2} \cdots \mathbf{u}_N\right] \tag{3.17}$$

where the columns of $\mathbf{U}_s$ are the $P$ eigenvectors associated with the largest eigenvalues of $\mathbf{C}$. The columns of $\mathbf{U}_s$ form a set of basis vectors of the signal subspace, that is, the subspace spanned by constituting signals in $\mathbf{C}$. Hence, all the constituting signals are orthogonal to noise subspace, providing the basic measure for user identification. In a symbol-synchronous DS-CDMA, if the spreading waveforms of active users are known, active users can be distinguished by projecting each signature sequence $\mathbf{s}_i$ vector onto the noise and signal subspaces [25],

$$f_k = \left(\mathbf{s}_k^T \mathbf{U}_n\right)\left(\mathbf{s}_k^T \mathbf{U}_n\right)^T = \left\|\mathbf{s}_k^T \mathbf{U}_n\right\|^2 \tag{3.18}$$

$$g_k = \left(\mathbf{s}_k^T \mathbf{U}_s\right)\left(\mathbf{s}_k^T \mathbf{U}_s\right)^T = \left\|\mathbf{s}_k^T \mathbf{U}_s\right\|^2 \tag{3.19}$$

If $\mathbf{s}_k$ belongs to an active user, it lies in the signal subspace and then $f_k$ is equal to zero. So, if $f_k$ is not equal to zero, it indicates that the user corresponding to $\mathbf{s}_k$ is not active at this moment. By the same principle, if the $k_{th}$ user is active, $\mathbf{s}_k$ resides in the signal subspace and $g_k$ will be equal to one. However the approach cannot be directly applied when spreading waveforms are not known and it becomes even more involved for a symbol-asynchronous case.

## *3-4. Blind Spreading Waveform Discovery and Identification*

In this section, the approach for blind spreading waveform discovery and user identification is presented. In the following, the scheme is first proposed for a synchronous CDMA model and then later its application is extended to the asynchronous case.

## 3-4.1. *Synchronous DS-CDMA*

Assuming that users are all synchronized and their timings are known to the receiver, i.e., $m_k$=0, we have,

$$\mathbf{D}_{m_k}^{p} = [\mathbf{0}]_{N\times N} \tag{3.20}$$

$$\mathbf{D}_{m_k}^{c} = \mathbf{I}_{N\times N} \tag{3.21}$$

and, consequently

$$\mathbf{S} = [\mathbf{0} \quad \mathbf{s}_1 \quad \mathbf{0} \quad \mathbf{s}_2 \quad \cdots \quad \mathbf{0} \quad \mathbf{s}_K]_{N\times 2K} \tag{3.22}$$

In a non-cooperative case, where the signature sequences of the users are not known, we have to examine the orthogonality of **S** and the noise subspace for all combinations of spreading waveforms. Since the spreading code is comprised of $N$ chips, this examination calls for a complete search over $2^{N-1}$ different possible combinations of chips in a spreading code.

If there are $K$ active users in a system, depending on the cross-correlations between the active codes and also the set threshold for Equations (3.18)-(3.19), signal projection may not only result in all the active spreading codes in Equation (3.22), but also in falsely declaring their linear combinations. That is simply because the linear combinations of the codes will also satisfy

$$f_i \approx 0 \tag{3.23}$$

$$g_i \approx 1. \tag{3.24}$$

Therefore, instead of $K$, we may obtain $K'$ mixed solutions ($K < K' < 2^{N-1}$). Depending on the value of $K$ and the selected thresholds for detection in Equations (3.18)-(3.19), $K'$ might be several times larger than $K$. Since the received signal **r** is comprised of only $K$

authentic spreading codes, in order to resolve the ambiguity and distinguish between the authentic and false solutions, we have to somehow inspect the relation of each solution to **r**. The approach is as follows. For every solution resulting from the initial signal projection, we apply a transformation based on that solution on the received signal and then inspect the statistics of the results. The transformation has to be able to separate different users' signals to avoid their statistics being mixed up. A proper choice for this task is to use a decorrelating transformation. This does not seem possible since the spreading codes are not known yet. Assuming prior knowledge of signature sequences, in a symbol-synchronous CDMA system, a decorrelator receiver can be devised only based on signal subspace information for each active user [28]. In this case all the $K'$ solutions resulting from the signal projection, can be regarded as a-priori known signature sequences and since the signal subspace information is already available from the first step, one can proceed to implement the decorrelator receiver $\mathbf{d}_i$ for each of the candidate solutions

$$\mathbf{d}_i = \mu_i \mathbf{U}_s \left(\mathbf{\Lambda}_s - \sigma^2 \mathbf{I}_K\right)^{-1} \mathbf{U}_s^T \mathbf{s}_i \qquad 1 \le i \le K' \tag{3.25}$$

where $\mu$ is a non-zero normalizing factor [28].

$$\mu_i = \frac{1}{\mathbf{s}_i^T \mathbf{U}_s \left(\mathbf{\Lambda}_s - \sigma^2 \mathbf{I}_K\right)^{-1} \mathbf{U}_s^T \mathbf{s}_i} \tag{3.26}$$

Depending on the nature of $\mathbf{s}_i$, application of Equation (3.25) to the received signal produces different results. If $\mathbf{s}_i$ is an authentic solution, then $\mathbf{d}_i$ represents a single decorrelating function similar to the Equation (3.25).

$$\mathbf{d}_i = \mu_i \mathbf{U}_s \left(\mathbf{\Lambda}_s - \sigma^2 \mathbf{I}_K\right)^{-1} \mathbf{U}_s^T \mathbf{s}_i \qquad 1 \le i \le K' \tag{3.27}$$

However, if $\mathbf{s}_i$ is not an authentic solution, i.e., if it has resulted from a linear combination of active codes, then $\mathbf{d}_i$ will be a linear combination of decorrelating functions of the active codes.

$$\mathbf{s}_i = \sum_{j=1}^{K} \alpha_j \mathbf{s}_j \tag{3.28}$$

where $\alpha_j$'s are real numbers representing the combining factors. Thus, the decorrelating transform is

$$\begin{aligned} \mathbf{d}_i &= \mu_i \mathbf{U}_s \left(\Lambda_s - \sigma^2 \mathbf{I}_K\right)^{-1} \mathbf{U}_s^T \sum_{j=1}^{K} \alpha_j \mathbf{s}_j \\ &= \mu_i \sum_{j=1}^{K} \alpha_j \frac{\mathbf{d}_j}{\mu_j} \end{aligned} \tag{3.29}$$

where

$$\begin{aligned} \mu_i &= \frac{1}{\left(\sum_{j=1}^{K} \alpha_j \mathbf{s}_i^T\right) \mathbf{U}_s \left(\Lambda_s - \sigma^2 \mathbf{I}_K\right)^{-1} \mathbf{U}_s^T \left(\sum_{l=1}^{K} \alpha_l \mathbf{s}_l\right)} \\ &= \frac{1}{\sum_{j=1}^{K} \sum_{l=1}^{K} \alpha_j \alpha_l \mathbf{s}_j^T \mathbf{U}_s \left(\Lambda_s - \sigma^2 \mathbf{I}_K\right)^{-1} \mathbf{U}_s^T \mathbf{s}_l} \\ &= \frac{1}{\sum_{j=1}^{K} \sum_{l=1}^{K} \frac{\alpha_j \alpha_l}{\mu_l} \mathbf{s}_j^T \mathbf{d}_l} = \frac{1}{\sum_{j=1}^{K} \frac{\alpha_j^2}{\mu_j}} \end{aligned} \tag{3.30}$$

By applying Equation (3.25) to the received signal, we have

$$\begin{aligned} z_i &= \mathbf{d}_i^T \mathbf{r} = \mathbf{d}_i^T \mathbf{S} \mathbf{A} \mathbf{b} + \mathbf{d}_i^T \mathbf{n} \\ &= \mathbf{d}_i^T \mathbf{S} \mathbf{A} \mathbf{b} + w_i \end{aligned} \tag{3.31}$$

where $w_i$ is white Gaussian noise with a variance $\sigma_{w_i}^2 = \left(\mathbf{d}_i^T \mathbf{d}_i\right)\sigma^2$. In either case, application of Equation (3.27) or (3.29) results in noise enhancement. The results of

decorrelating transforms operating on the data part of Equation (3.31) are significantly different.

$$z_i = \begin{cases} A_i b_i + w_i & \text{where } \mathbf{s}_i \text{ is a single code} \\ \mu_i \sum_{j=1}^{K} \frac{\alpha_j}{\mu_j} A_j b_j + w_i & \text{where } \mathbf{s}_i \text{ is a linear combination of codes} \end{cases} \tag{3.32}$$

Figures 3.2 and 3.3 show the histograms of $z_i$ based on 5000 samples for the two cases of authentic and false solutions. The distinct difference between the two cases lies in their probability density functions. For the case where $\mathbf{s}_i$ is an authentic solution, samples at the decorrelator output are clustered about the $\pm A_i$. In Figure 3.2, the only source of perturbation of the samples is the additive noise; interference from other codes does not exist. However, when the $\mathbf{s}_i$ is a false solution, resulting samples are dispersed significantly. The amount of the dispersion depends on the number of constituting codes, corresponding data bits, combining factors and users' amplitudes.

Based on this difference, we define a cost function $J(\mathbf{d}_i)$ that measures the deviation from the average of the absolute value of the decorrelation results.

$$J(\mathbf{d}_i) = \left| \frac{E\left(z_i^{\,2}\right)}{E^2\left(|z_i|\right)} - 1 \right| \tag{3.33}$$

where $E(\,)$ denotes the expected value of the produced samples over all possible noise and data sequences. Another way to interpret the definition of this cost function is the following. The main difference between the two cases of a false or authentic solution is how the power of the signal is distributed over the amplitude samples. In the case of an authentic solution, the power is mainly concentrated over a small range of amplitudes in the vicinity of the mean absolute amplitude. However, in the case of a false solution, the values are irregularly spread over a wide range of samples. Hence, the difference between

the total power and the power of the mean absolute amplitude can be used to distinguish the two cases.

$$J(\mathbf{d}_i) = \left| \frac{P_{Total}}{P_{Av.Abs.Amp.}} - 1 \right| = \left| \frac{E\left(z_i^{\,2}\right)}{E^2\left(|z_i|\right)} - 1 \right| \tag{3.34}$$

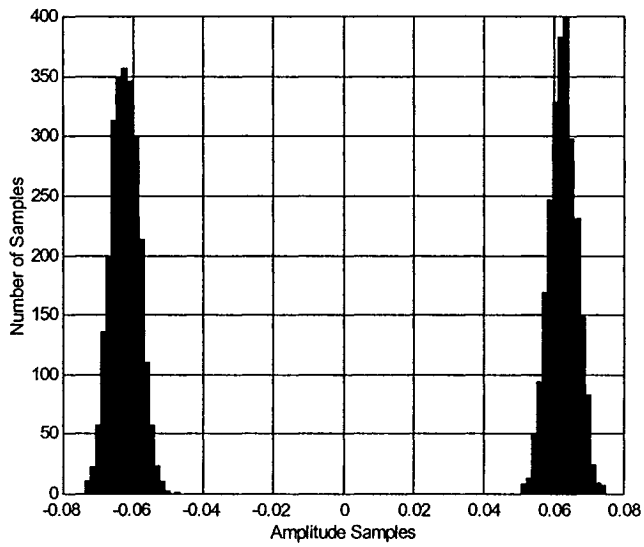


**Figure 3.2 Histogram showing the probability density function of the produced samples for an authentic solution**

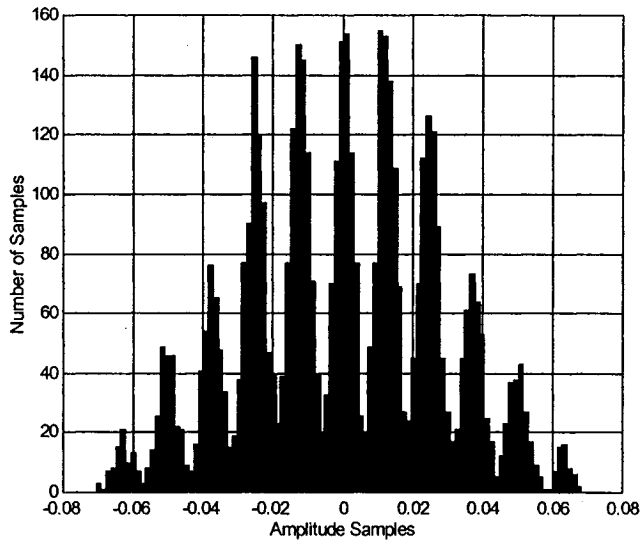


**Figure 3.3 Histogram showing the probability density function of the produced samples for a false solution**

Thus, we decide in favor of $\mathbf{s}_i$ as an authentic solution if the corresponding $\mathbf{d}_i$ results in a small value in Equation (3.33). In other words, we seek for the solution,

$$\mathbf{s}_k = \arg\max_{\mathbf{s}_k} \frac{1}{J(\mathbf{d}_k)}. \tag{3.35}$$

Now, let's take a deeper look at the two cases of authentic and false solutions. If $\mathbf{s}_i$ is an authentic solution then,

$$z_i = A_i b_i + w_i \tag{3.36}$$

$$p(z_i) = \frac{1}{2\sqrt{2\pi}\sigma_{w_i}} \exp\left(\frac{-(z_i + A_i)^2}{2\sigma_{w_i}^2}\right) + \frac{1}{2\sqrt{2\pi}\sigma_{w_i}} \exp\left(\frac{-(z_i - A_i)^2}{2\sigma_{w_i}^2}\right). \tag{3.37}$$

where $p(z_i)$ is the probability density function of the decorrelator output $z_i$. Now, assuming $A_i >> \sigma_{w_i}$,

$$p(|z_i|) \approx \frac{1}{\sqrt{2\pi}\sigma_{w_i}} \exp\left(\frac{-(|z_i| - A_i)^2}{2\sigma_{w_i}^2}\right) \tag{3.38}$$

then we have,

$$J(\mathbf{d}_i) = \left|\frac{E(z_i^2)}{E^2(|z_i|)} - 1\right| = \left|\frac{A_i^2 + \sigma_{w_i}^2}{A_i^2} - 1\right| = \frac{\sigma_{w_i}^2}{A_i^2} \tag{3.39}$$

Now, we consider the case when $\mathbf{s}_i$ is a false solution. In this case, since the interference from the other codes is the dominant contributor to the dispersion, the additive noise is much less significant.

$$z_i = \mu_i \sum_{j=1}^{K} \frac{\alpha_j}{\mu_j} A_j b_j + w_i \tag{3.40}$$

The probability density function of $z_i$ is a function of the combining factors, the receive amplitudes and the information bits of interfering users. Therefore, a closed form general

derivation does not seem to be easy to find. For a special case where there are many active users, the probability density function $p(z_i)$ can be approximated as a zero mean Gaussian distribution by using the central limit theorem.

$$p(z_i) = \frac{1}{\sqrt{2\pi}\sigma_{z_i}} \exp\left(\frac{-z_i^2}{2\sigma_{z_i}^2}\right) \tag{3.41}$$

where

$$\sigma_{z_i}^2 = \sum_{j=1}^{K}\left(\frac{\mu_i}{\mu_j}\alpha_j A_j\right)^2 + \sigma_{w_i}^2 . \tag{3.42}$$

Then the mean of the absolute amplitude is

$$E(|z_i|) = 2\int_0^{+\infty} z_i p(z_i) = \sqrt{\frac{2}{\pi}}\sigma_{z_i} . \tag{3.43}$$

Now the cost function for a false solution can be approximated to

$$J(\mathbf{d}_i) = \left|\frac{E(z_i^2)}{E^2(|z_i|)} - 1\right| = \left|\frac{\sigma_{z_i}^2}{\frac{2}{\pi}\sigma_{z_i}^2} - 1\right| = \frac{\pi - 2}{2} . \tag{3.44}$$

As Equation (3.40) shows, even if the noise is removed, the interference term will still remain. The only way to remove the interference term and to make Equation (3.39) insignificant is to have all the combining factors $\alpha_j$=0 for $i \neq j$, but this contradicts the assumption of a false solution.

## *3-4.2. Asynchronous DS-CDMA*

In a real system, users are not always symbol-synchronized and there is some amount of delay between any two users. There are several reasons for the delay. In applications

where users initiate and drop their calls without coordination, a random delay between the signals is inevitable. Even if the calls become coordinated, due to the fact that users have different locations, their signals travel different paths and may experience several chips delay relative to each other.

Now let's consider an asynchronous system. In such a system, the receiver does not know the timing of users. Consequently, the collection window has to start from an arbitrary point that could be at the middle of a received bit. For the $i_{th}$ bit interval, if we ignore the noise term, the contribution of the $k_{th}$ user to the received signal is

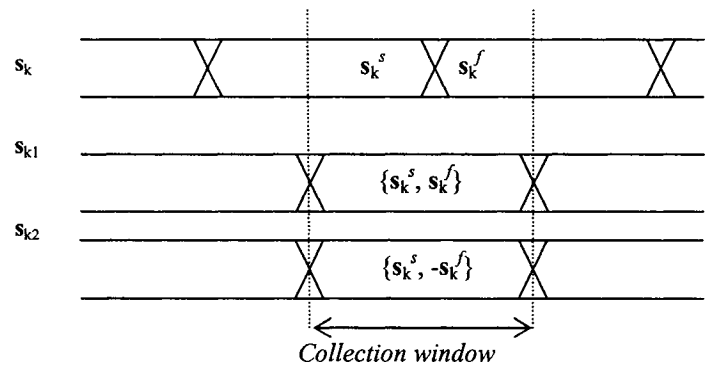


**Figure 3.4 The equivalent synchronous model of a two asynchronous users**

$$\mathbf{r}_k(i) = A_k e^{j\theta_k} \left\{ b_k^{i-1} \mathbf{D}_{m_k}^{p} + b_k^{i} \mathbf{D}_{m_k}^{c} \right\} \mathbf{s}_k . \tag{3.45}$$

Figure 3.4 shows the effective spreading waveforms for the $k_{th}$ user. In the Figure 3.4, superscript $^f$ and $^s$ denote the first and second portion of the spreading waveform, as the collection window partitions it. Since $b_k^{i-1}, b_k^{i} \in \{\pm 1\}$, the effective spreading waveform from the receiver point of view is either

$$\mathbf{s}_{k_1} = \left\{ \mathbf{D}_{m_k}^{p} + \mathbf{D}_{m_k}^{c} \right\} \mathbf{s}_k \tag{3.46}$$

or,

$$\mathbf{s}_{k_2} = \left\{\mathbf{D}^{p}_{m_k} - \mathbf{D}^{c}_{m_k}\right\}\mathbf{s}_k. \tag{3.47}$$

Therefore, by performing EVD and waveform projection onto the signal and noise subspaces, the effective spreading waveforms for the $k_{th}$ user will be found as Equations (3.46)-(3.47). Now, if we implement decorrelating transforms corresponding to each of the effective spreading waveforms, based on the property of the decorrelating transform we will have

$$\mathbf{d}_{k_1}{}^{T}\mathbf{s}_{k_1} = 1, \quad \text{but} \quad \mathbf{d}_{k_1}{}^{T}\mathbf{s}_{k_2} = 0 \tag{3.48}$$

$$\mathbf{d}_{k_2}{}^{T}\mathbf{s}_{k_2} = 1, \quad \text{but} \quad \mathbf{d}_{k_2}{}^{T}\mathbf{s}_{k_1} = 0. \tag{3.49}$$

but since the collection window is assumed to be not synchronous with the $k_{th}$ user, its information bit will be toggling during the decorrelation and therefore

$$\mathbf{d}_{k_1}{}^{T}\left\{b_k^{i-1}\mathbf{D}^{p}_{m_k} + b_k^{i}\mathbf{D}^{c}_{m_k}\right\}\mathbf{s}_k \neq 0 \tag{3.50}$$

$$\mathbf{d}_{k_2}{}^{T}\left\{b_k^{i-1}\mathbf{D}^{p}_{m_k} + b_k^{i}\mathbf{D}^{c}_{m_k}\right\}\mathbf{s}_k \neq 0 \tag{3.51}$$

Thus, the decorrelation process is successful only if the candidate spreading waveform belongs to a user that is synchronous to the collection window,

$$\mathbf{D}^{p}_{m_k} = 0 \tag{3.52}$$

$$\mathbf{d}_k{}^{T}\mathbf{s}_k = 1, \quad \text{but} \quad \mathbf{d}_k{}^{T}\mathbf{s}_{l_{1,2}} = 0 \quad (l \neq k) \tag{3.53}$$

Thus, we can jointly estimate the spreading waveform and timing of active users by simply extending the dimension of the search in (3.35). Then, the argument that maximizes the following, results in joint discovery of spreading waveform and timing of active users,

$$\begin{bmatrix}\mathbf{s}_k \\ \tau_k\end{bmatrix} = \arg\max_{\mathbf{s}_k,\tau_k} \frac{1}{J(\mathbf{d}_k)}. \tag{3.54}$$

that requires the search to be performed over both waveform and time domains.

After finding the active spreading codes, user identification will be completed by estimating the users' power. An estimate of the users' powers can be obtained from Equation (3.11) as follows

$$\mathbf{A}\mathbf{A}^T = \left(\mathbf{S}^T\mathbf{S}\right)^{-1}\mathbf{S}^T\left(\mathbf{C}-\sigma^2\mathbf{I}_N\right)\mathbf{S}\left(\mathbf{S}^T\mathbf{S}\right)^{-1}, \tag{3.55}$$

or, equivalently

$$\mathbf{A}\mathbf{A}^T = \mathbf{R}^{-1}\mathbf{S}^T\left(\mathbf{C}-\sigma^2\mathbf{I}_N\right)\mathbf{S}\mathbf{R}^{-1}, \tag{3.56}$$

where $\sigma^2$ is estimated from the initial subspace decomposition. Also, instead of a group estimation of powers, a given user's power can be independently estimated as

$$A_i^2 = E\left(z_i^2\right) - \sigma_{w_i}^2 = E\left(z_i^2\right) - \left(\mathbf{d}_i^T\mathbf{d}_i\right)\sigma^2. \tag{3.57}$$

## 3-5. *Flow-graph of the proposed scheme*

The approach can be summarized as shown in Figure 3.5. The collection of the samples of the received signal can be started from an arbitrary point in time. An EVD on **C** is performed to decompose the signal and noise subspaces. Then, Equation (3.18) and Equation (3.19) are examined for the entire $2^{N-1}$ possible combinations of spreading sequences and reject $\mathbf{s}_k$'s that do not satisfy orthogonality condition between signal and noise subspaces. For the sequences that satisfy Equation (3.18) and Equation (3.19), then Equation (3.33) is evaluated.

If $J(\mathbf{d}_k)^{-1}$ is a large value, it implies a low dispersion of the decorrelation results and consequently, the corresponding spreading waveform belongs to an active user who shares the same timing as the collection window. Thus, in order to estimate the delay for

all users, we have to slide the collection window by one chip interval $T_c$ at a time and repeat all the evaluations.

For an asynchronous system with a processing rate of $N$, to complete the search in time, $N$ shift is required to cover the entire bit interval. This indicates an order of complexity of $2^{N-1} \times N$ for a complete identification.

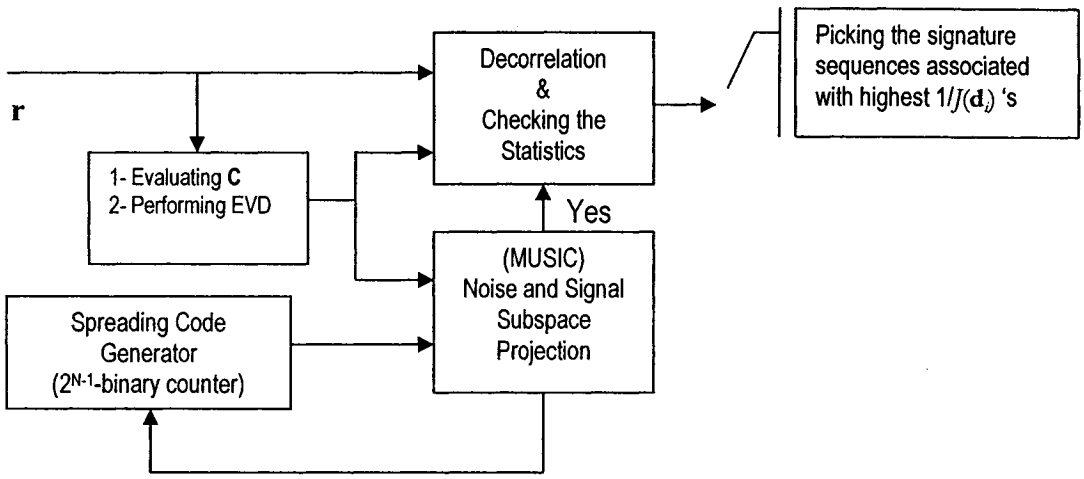


**Figure 3.5 The flow-graph of the proposed algorithm**

## *3-6. Simulations*

Here some simulation results are presented to demonstrate the capability and the performance of the proposed scheme. Through out the simulations, a processing gain of $N$=16 is assumed, unless specified otherwise. User's signal strength and noise power are set according to each simulation scenario. The accumulation length for the evaluation of the autocorrelation matrix, $L_1$, and the observation length for inspecting the statistics of $z_i$, $L_2$, are $L_1$=5000 and $L_2$=500 samples, respectively. Since the spreading codes are not

available in advance, signature sequences are generated by a $2^{N-1}$ counter and then projected onto the subspaces.

Figure 3.6 shows the Quadrature components of the decorrelated received signal as expressed in Equation (3.31). Figures 3.6a and 3.6b show the decorrelation results for two different false solutions. In each case, results indicate a high degree of dispersion that is exploited for eliminating that candidate. As shown in Figures 3.6a and 3.6b, the distribution of samples for false solutions can be different from each other, however it always demonstrate some form of dispersion.

Figure 3.7 shows the results for an authentic solution. In the case of the authentic solution, the produced samples exhibit much less dispersion that makes the solution very distinct from a false solution. Evaluation of the Equation (3.33) for such solution indicates a high value.

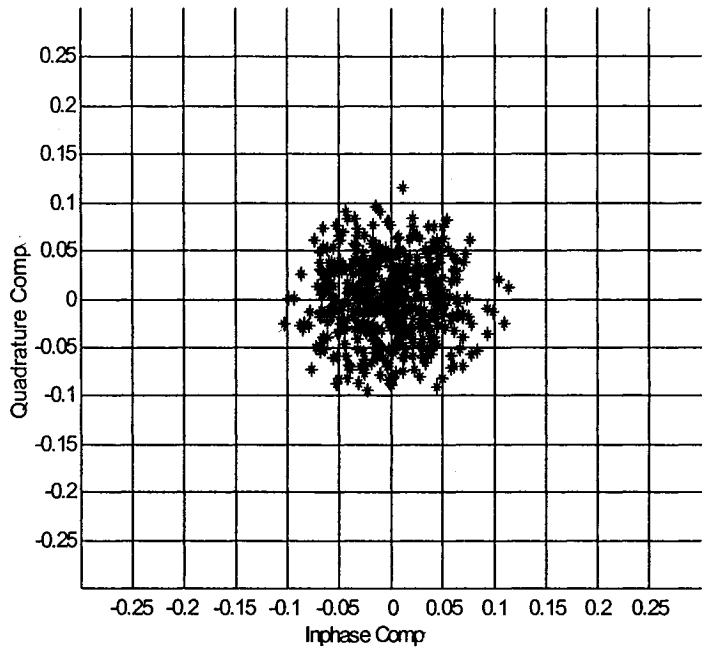


**(a)**

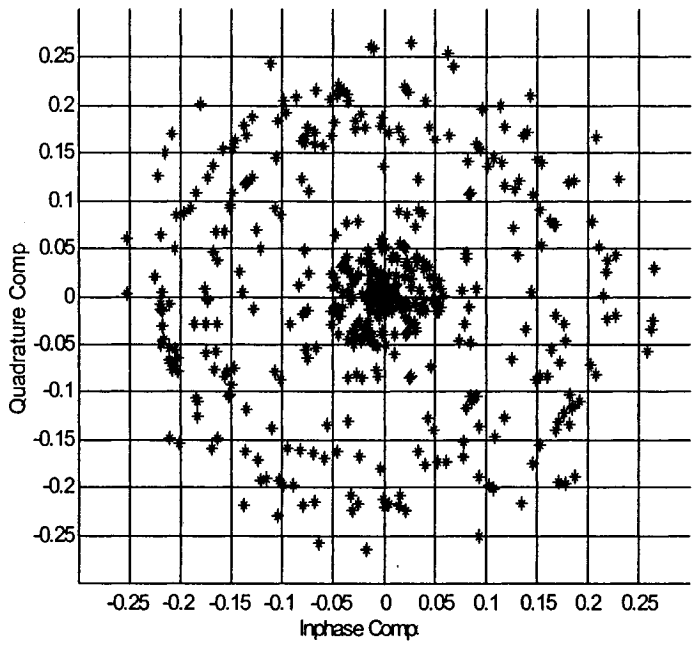


**(b)**

**Figure 3.6 Decorrelation results from false solutions (a), (b)**

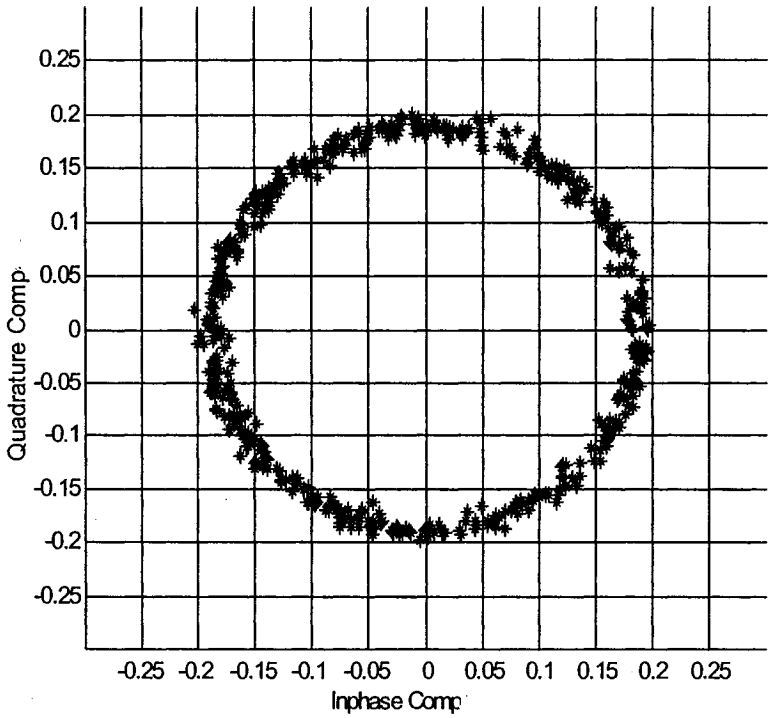


**Figure 3.7 Decorrelation results from an authentic solution**

Figure 3.8 shows the results of blind identification in a synchronous DS-CDMA model. The processing gain $N$=16, and there are 10 active users operating in the system. The receiver has no advance knowledge of the spreading waveforms and the activity of the users. The vertical axis represents the inverse of the cost function value for each candidate solution, and the horizontal axis represents the index number corresponding to each waveform. Two different power scenarios are considered. Figure 3.8a demonstrates the results for the case where all the 10 users have equal power with an SNR of 30 dB.

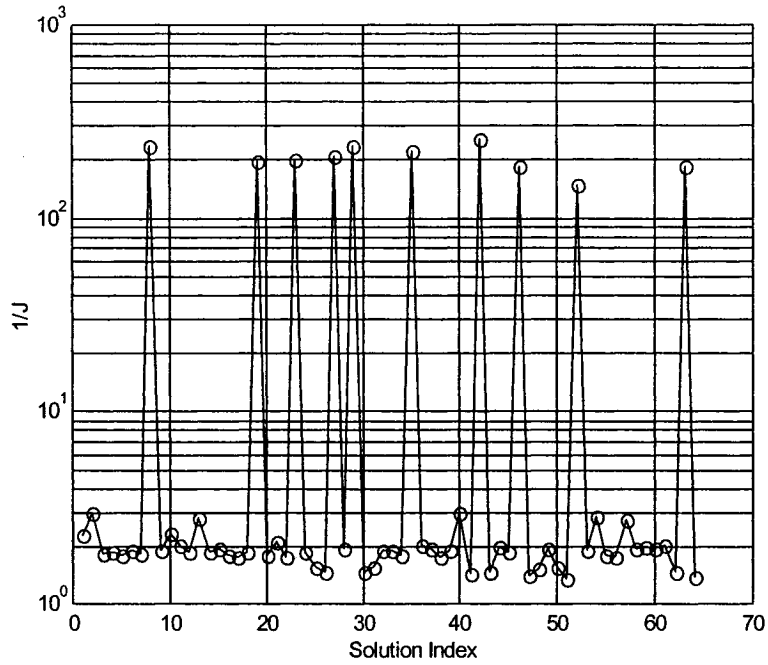


(a)

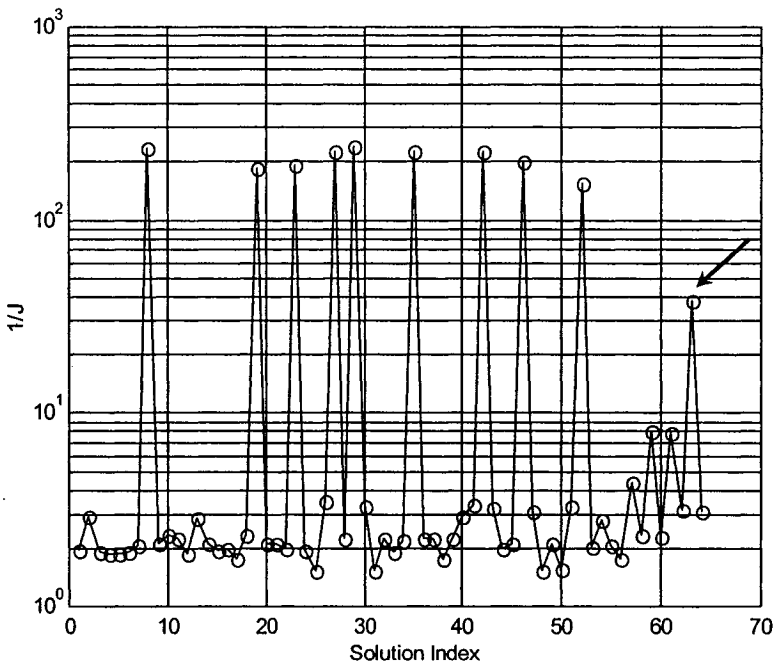


(b)

**Figure 3.8 Plots of 1/J for all the candidate solutions, (a) – Equal power users with SNR=30 dB, (b) – Unequal power users, one user with SNR=20 dB and all others with SNR=30 dB**

From the $2^{N-1}=2^{15}$ possible choices for the spreading waveforms, subspace signal and noise projection identifies only 64 candidate solutions. Evaluation of the cost function (3.33) reveals the 10 authentic solutions as shown in Figure 3.8a. For the next simulation, a worst-case scenario of power balance is considered. It is assumed that there are 9 equal power users with an SNR of 30dB, and the $10^{th}$ user is weaker by 10 dB, having an SNR=20dB. Figure 3.8b shows the identification results for this condition. In Figure 3.8b, the solution corresponding to the weak user is shown by an arrow. It is worthwhile to note that even the solution associated with the weak user exhibits a strong peak compared to the false solutions. From Figure 3.8, two observations in conjunction with Equations (3.39) and (3.44) can be made. As estimated earlier, the value of the cost function for false solutions approaches Equation (3.44). Also, as stated in Equation (3.39), for authentic solutions, $J(\mathbf{d}_k)^{-1}$ is proportional to the user's power.

Figure 3.9 shows the estimation error $(\sigma_{Ai}/ A_i)$ of the receive amplitude at various users' power scenarios. In this case, we assume that there are 8 active users in the system. After performing the identification, we estimate their powers. Users are grouped into one, two, four and eight equal power groups of equal powers with the following SNR's (in dB) at the receiver side

$$\mathbf{SNR} = [20 \;\; 26 \;\; 29.5 \;\; 32 \;\; 34 \;\; 35.5 \;\; 36.9 \;\; 38]$$
$$\mathbf{SNR} = [20 \;\; 20 \;\; 26 \;\; 26 \;\; 32 \;\; 32 \;\; 38 \;\; 38]$$
$$\mathbf{SNR} = [20 \;\; 20 \;\; 20 \;\; 20 \;\; 26 \;\; 26 \;\; 26 \;\; 26]$$
$$\mathbf{SNR} = [20 \;\; 20 \;\; 20 \;\; 20 \;\; 20 \;\; 20 \;\; 20 \;\; 20]$$

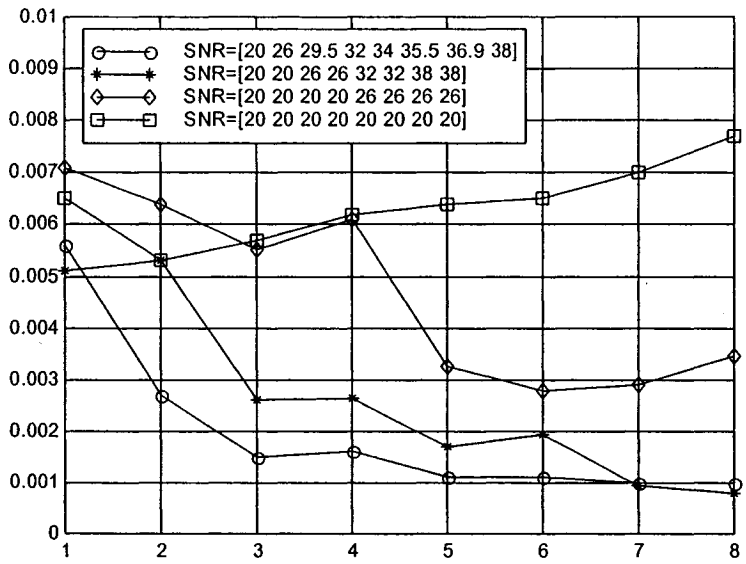


**Figure 3.9 Users' power estimation error for different users' power scenario**

As demonstrated in Figure 3.9, in any scenario, the estimation error for users with the highest SNR is very low. Also, it should be noted that the estimation error for a user with a certain SNR is about the same in any users' power scenario. For example, the estimation error for users with a SNR of 20 dB, in any of the above scenarios, is in the same range of $5\times10^{-3}$ to $8\times10^{-3}$. Similarly, the estimation error for users with SNR of 38 dB is always in the vicinity of $1\times10^{-3}$. In other words, the estimation error is mainly a function of the signal to noise ratio of each user and the interference from other users does not have significant impact on it.

In the next simulation, we consider an asynchronous DS-CDMA system with a processing gain of N=8. There are 4 asynchronous users operating in the system. The goal is to identify their spreading waveforms as well as their relative timings. For an asynchronous system, we have to implement the Equation (3.54). Therefore, we start to collect samples of the received signal from an arbitrary point within a bit period. Then the

subspace decomposition is performed for signal projection and the cost function Equation (3.33) is evaluated for each candidate solution. We slide the collection window N times, every time by one chip period $T_c$, and repeat the process again. In other words, to realize Equation (3.54), we implement Equation (3.33) $N$ times, and every time we start to collect samples from a new point. Figure 3.10 and 3.11 show the simulation results. In Figure 3.10 and 3.11, we have the new dimension represented by "Relative Delays" which signifies the results of cost function evaluation for different starting points of the collection window. Figure 3.10 shows the result for the case where all four users have equal power with an SNR of 30 dB. However, Figure 3.11 exhibits the results for the case where there is a weak user and the other three users have equal power, each 10 dB stronger than the weak user. As Figure 3.10 and 3.11 demonstrate, in both cases, four users with relative delays of $T_c$, $4T_c$, $6T_c$, $7T_c$ are identified. Similar to the synchronous case, there is a higher margin for detection when a user has a high power. Nevertheless, for the unequal power case, the margin for correct detection is still high enough. In Figure 3.11, the arrow points to the solution corresponding to the weak user.

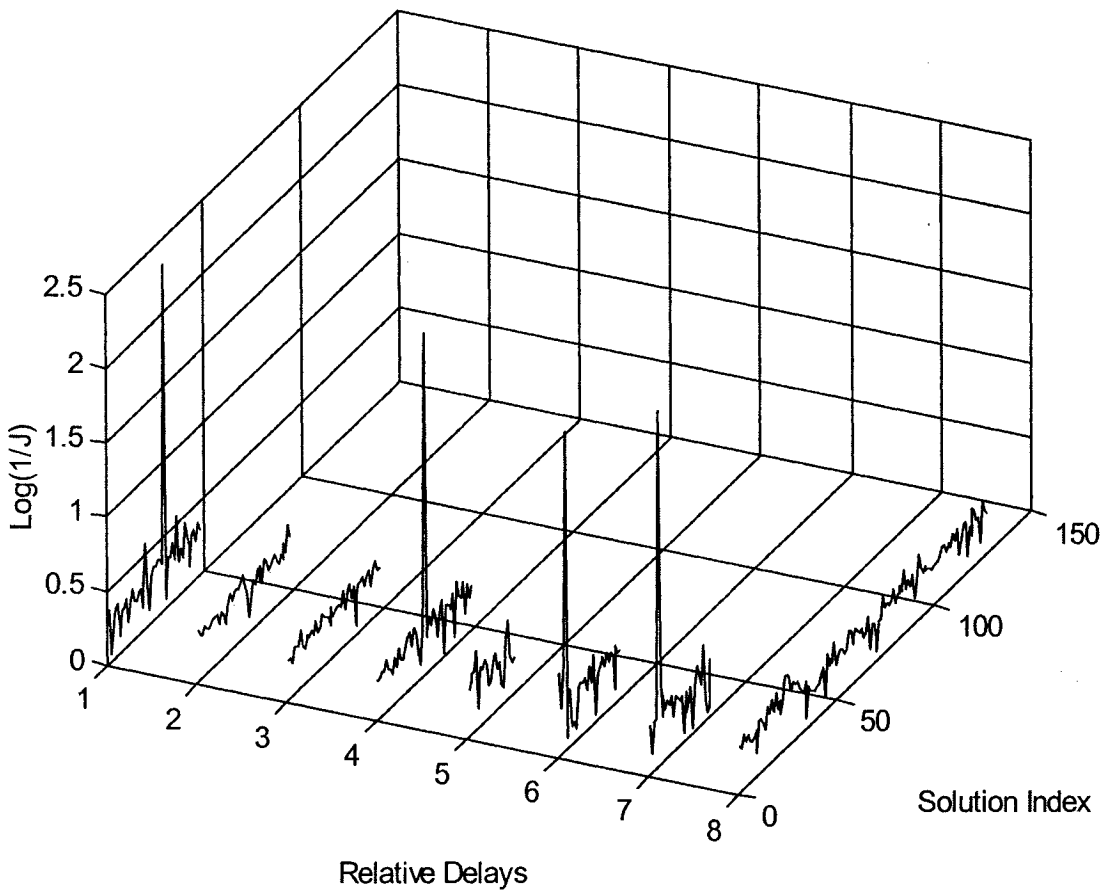


**Figure 3.10 Plots of 1/J for an asynchronous model for equal power users with SNR=30 dB**

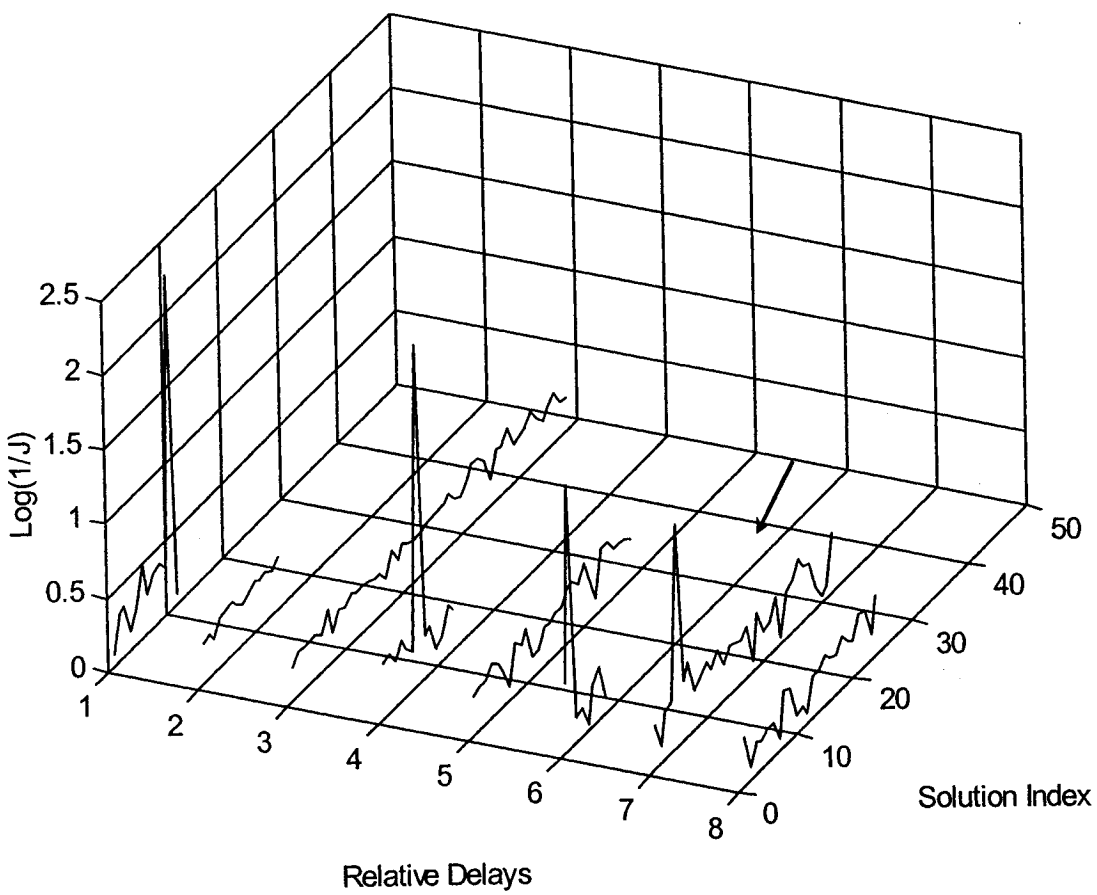


**Figure 3.11 Plots of 1/J for an asynchronous model for unequal power users, one user with SNR=20 dB and others with SNR=30 dB.**

## *3-5. Concluding Remarks*

In this chapter, we presented a novel scheme for blind identification of active users and timing estimation for a symbol-asynchronous DS-CDMA system. The main feature of the proposed approach is that it does not require any prior knowledge of users' parameters or any training sequence. By exploiting subspace signal decomposition, the proposed approach is able to discover the spreading waveform as well as the relative delays of the active users. The defined cost function resolves the ambiguity originating from the false solutions. The scheme is applicable to both synchronous and asynchronous systems. The simulation results indicate the robustness of the scheme in various users' power as well as channel scenarios.

# *Chapter 4*

# *Performance Evaluation*

## *4-1. Introduction*

This chapter presents the performance evaluation of the proposed algorithm under various conditions. These conditions cover main practical aspects such as: channel scenarios and computational load. In a multiuser environment, users' signals travel different paths and arrive at the receiver from different directions with different powers. Therefore, the channel can behave as a simple AWGN channel or take on a more complex fading model.

Also, in a dynamic CDMA channel, it is vital to minimize the computational complexity to match the dynamics of the users. Reduction of computational task can be accomplished by using various techniques such as: restricting the search, reducing the

observation intervals as well as efficient evaluation of autocorrelation matrix in asynchronous systems. Each proposed method is discussed and simulation results are presented.

A meaningful way to evaluate the performance of a detection block is by measuring the probability of false and missed detections. So, the probability of false and missed detection are evaluated and analytical as well as simulation results are presented.

Improving the accuracy in estimation of user's timing by employing over-sampling is also discussed. It is shown that by using over-sampling, the resolution of the timing estimation can be enhanced.

## *4-2. Reliability and Robustness of the Algorithm*

Before proceeding to performance evaluation analysis of the algorithm, it is worthwhile to investigate the consistency of the algorithm, which is very important in selection of the threshold. Figures 4-1, 4-2 and 4-3 show the simulation results for a system with a spreading factor of N=8 where 7 equal power users operate. The accumulation and the decorrelation length are $L_1$=2500 and $L_2$=250 symbols, respectively. For each SNR, the simulation was repeated 100 times to investigate the consistency of the general form of the results.

For the extreme case of low SNR=5dB, presented in Figure 4.1, the algorithm does not produce a consistent response. As a result, a significant number of misses as well as false detections can be expected. Figures 4-2 and 4-3 show the results for signal to noise ratios' of 15 dB and 25 dB, respectively. Both graphs exhibit a similar general form of the response, however, at high signal to noise ratio there is more margin between the floor

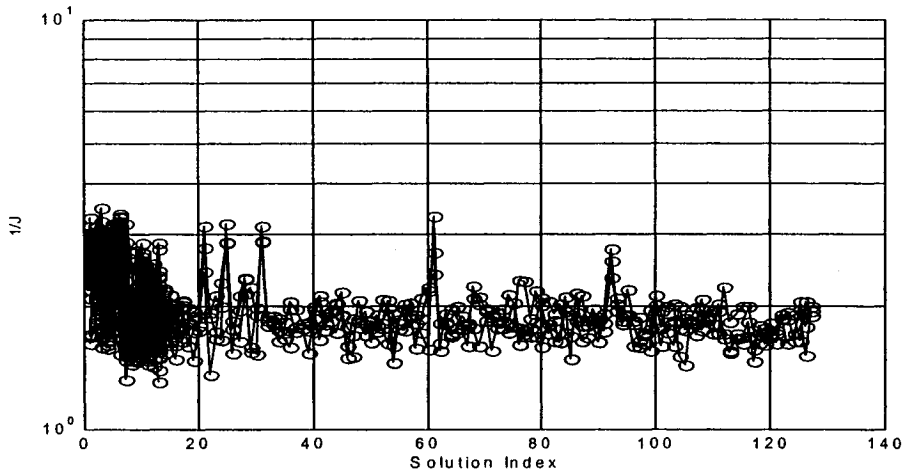


**Figure 4.1 Detection of 7 active equal power users, each with an SNR=5dB**

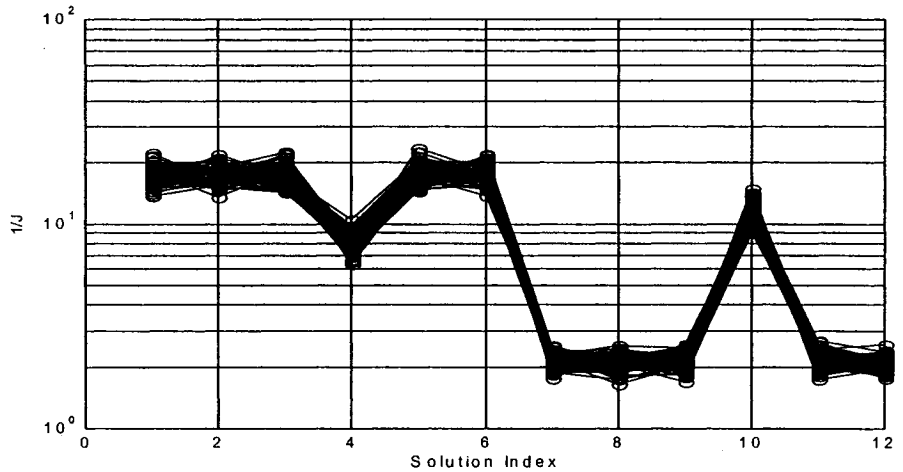


**Figure 4.2 Detection of 7 active equal power users, each with an SNR=15dB**

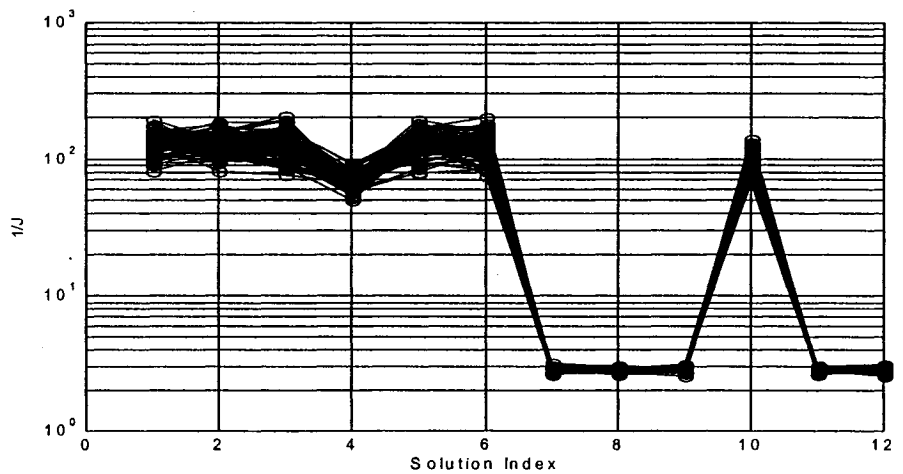


**Figure 4.3 Detection of 7 active equal power users, each with an SNR=25dB**

and the peaks. Thus, to avoid detection errors, the threshold has to be set according to the signal to noise ratio. Since the number of active users, $K$, becomes available from the subspace decomposition of the received signal, the threshold can be set iteratively. As such, the cost function is measured against a default threshold and then the results are compared to $K$. If the number of detected authentic solutions is lower than $K$, then the threshold is reduced further until $K$ authentic solutions are detected, and vice versa.

For the simulation results presented in Figures 4.2 and 4.3, confidence intervals corresponding to a certain confidence level can be estimated [33]. As an example, for the first peak associated to the first detected user, confidence intervals with a confidence level of 0.95 are measured. For a SNR=15 dB and SNR=25 dB, the estimated confidence intervals based on the measurement are $17.77 \pm 0.38$ and $147.90 \pm 2.46$, respectively. In both cases, the results confirm consistency of the algorithm.

## *4-3. Reducing the Processing Delay*

The algorithm presented in the previous chapter can be summarized as follows. The collection of the samples of the received signal can start from an arbitrary point. An EVD on $\mathbf{C}$ is performed to decompose the signal and noise subspaces. Then, we examine the orthogonality conditions for the entire $2^{N-1}$ possible combinations of spreading sequences and reject $\mathbf{s}_k$'s that do not satisfy the orthogonality between the signal and noise subspaces. For the remaining $\mathbf{s}_k$'s, the cost function is evaluated. A large $1/J(\mathbf{d}_k)$ implies a low dispersion of the decorrelation results and that, the corresponding spreading waveform belongs to an active user who has the same timing as the collection window. Thus, in order to estimate the delay for all the users, we have to slide the collection

window by one chip interval, $T_c$, at a time and repeat the same process all over again. In order to complete the search in time, $N$ shift is required to cover the entire bit interval. This indicates an order of complexity of $2^{N-1} \times N$ for complete identification.

For a dynamic communication environment, it is essential that the processing delay for detection of the active users be reduced. Thus, the followings initiatives are vital:

- optimization of the observation interval
- reduction in time and complexity involved in projection of $\mathbf{s}_k$'s onto the signal and noise subspaces,
- avoid repetition of sample collection to form **C** in an asynchronous system

## *4-3.1. Optimizing the Observation Interval*

In the following simulations, we investigate the effect of observation length on the detection process. In the simulations, 10 equal power users with SNR=30dB are assumed. Figure 4.4 presents the result for the effect of $L_1$, while $L_2$=500. In principle, $L_1$ has to be long enough to assure an accurate capture of the statistics of the received signal. Thus, in a system with $K$ active users, one may expect that $L_1$ should be several times larger than $2^K$. As Figure 4.4 shows, although $L_1$=50 causes significant reduction in detection margin, a value of $L_1$=500, while not being too long, can provide a reasonable margin for the detection. Since the length of $L_1$ is proportional to the number of active users, in practice the selection of $L_1$ can be done adaptively as follows. The process starts with a moderate value for $L_1$, and then by obtaining the number of active users from the subspace decomposition, $L_1$ can be adjusted for the next batch accordingly. For example, if the number of active users is found to be small, then $L_1$ can be shortened. On the other

hand, if $K$ is large, then $L_1$ should be increased for an accurate tracking of the users. Mainly, the effect of $L_1$ is on the accuracy of the subspace components. If $L_1$ is selected too low, the orthogonal properties of signal and noise are adversely affected, as shown in Figure 4.4a. The effect of $L_1$ on the accuracy of subspace components is thoroughly investigated in [32]. Therefore, we mainly focus on the effect of $L_2$.

Figure 4.5, shows the effect of $L_2$ on the detection process. $L_2$ can be selected significantly smaller than $L_1$, since $b_k$ takes only ±1. As Figure 4.5 demonstrates, the difference between $L_2$=100 and $L_2$=1000 seems to be negligible. Therefore, in order to acquire an accurate estimate of the statistics of $z_i$, $L_2$ might be only a few tens of bit periods long. Also, it is worth noting that the main difference between $L_2$=10 and $L_2$=100 is in the floor level of the plots. A higher value of $L_2$ results in a lower and a more uniform floor for the $J(\mathbf{d}_i)^{-1}$ plot. To summarize our observations from Figures 4-4 and 4-5, it can be concluded that the impact of $L_1$ is on the peaks and $L_2$ influences the floor level of the $J(\mathbf{d}_i)^{-1}$ plots.

In order to better appreciate the effect of $L_2$ on the performance of the proposed method, probability of false and missed detections should be measured. Figure 4.6, shows the probability of missed detection for a user with SNR=25 dB. The measurement is repeated for three different values of $L_2$. Basically, an $L_2$=10 is not acceptable, however the results start to be come reasonable only in the vicinity of $L_2$=1000 and higher. Figure 4.7 shows the measurement results for probability of false detection. It is assumed that there are 10 active equal power users in the system each with an SNR=25 dB. Similar to the previous case, an $L_2$=10 is too short and the result is not acceptable. However, unlike the previous case, $L_2$=100 and $L_2$=1000 show more consisting result.

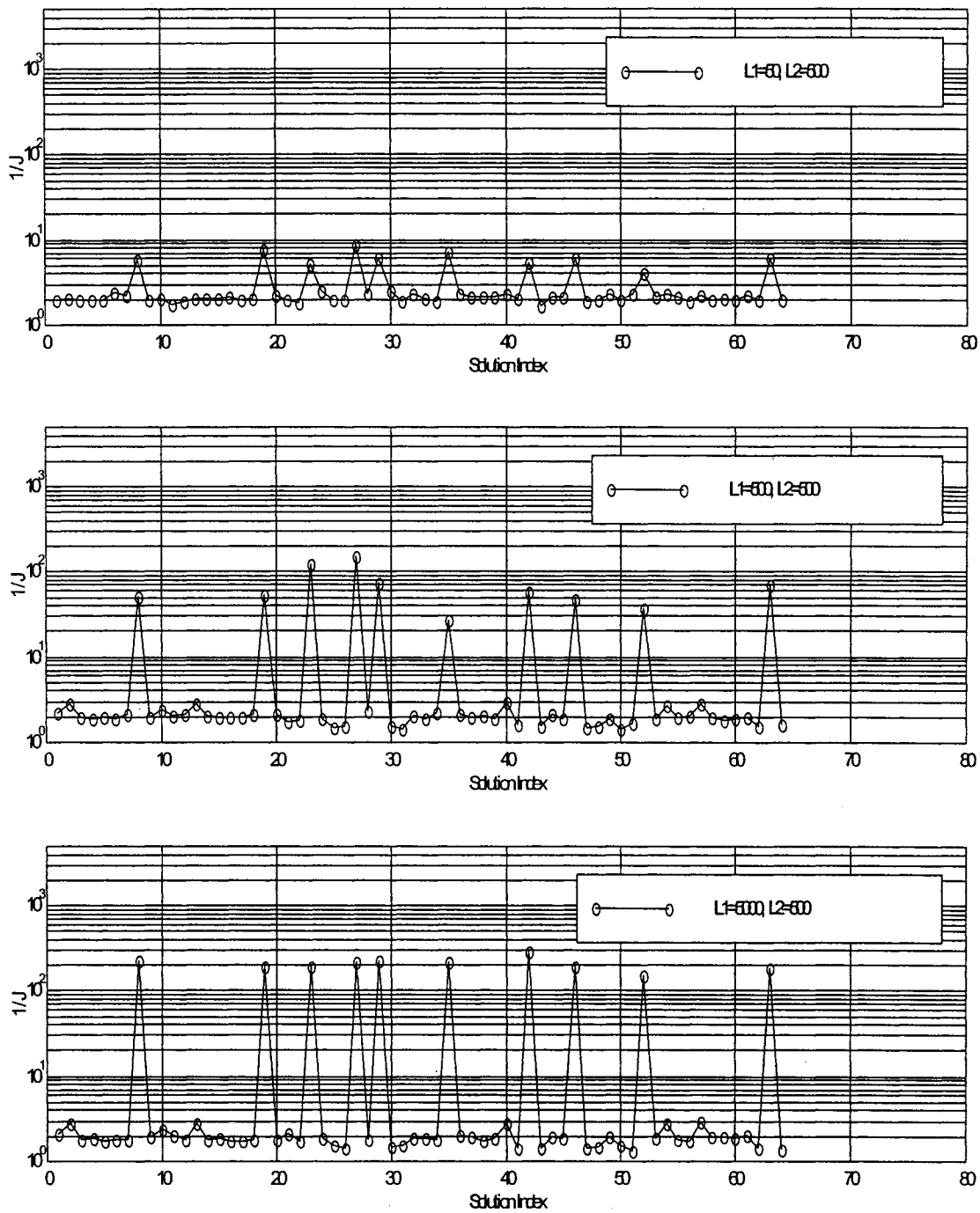


**Figure 4.4 Effect of $L_1$, the accumulation length required for evaluation of the autocorrelation matrix, on the detection process**

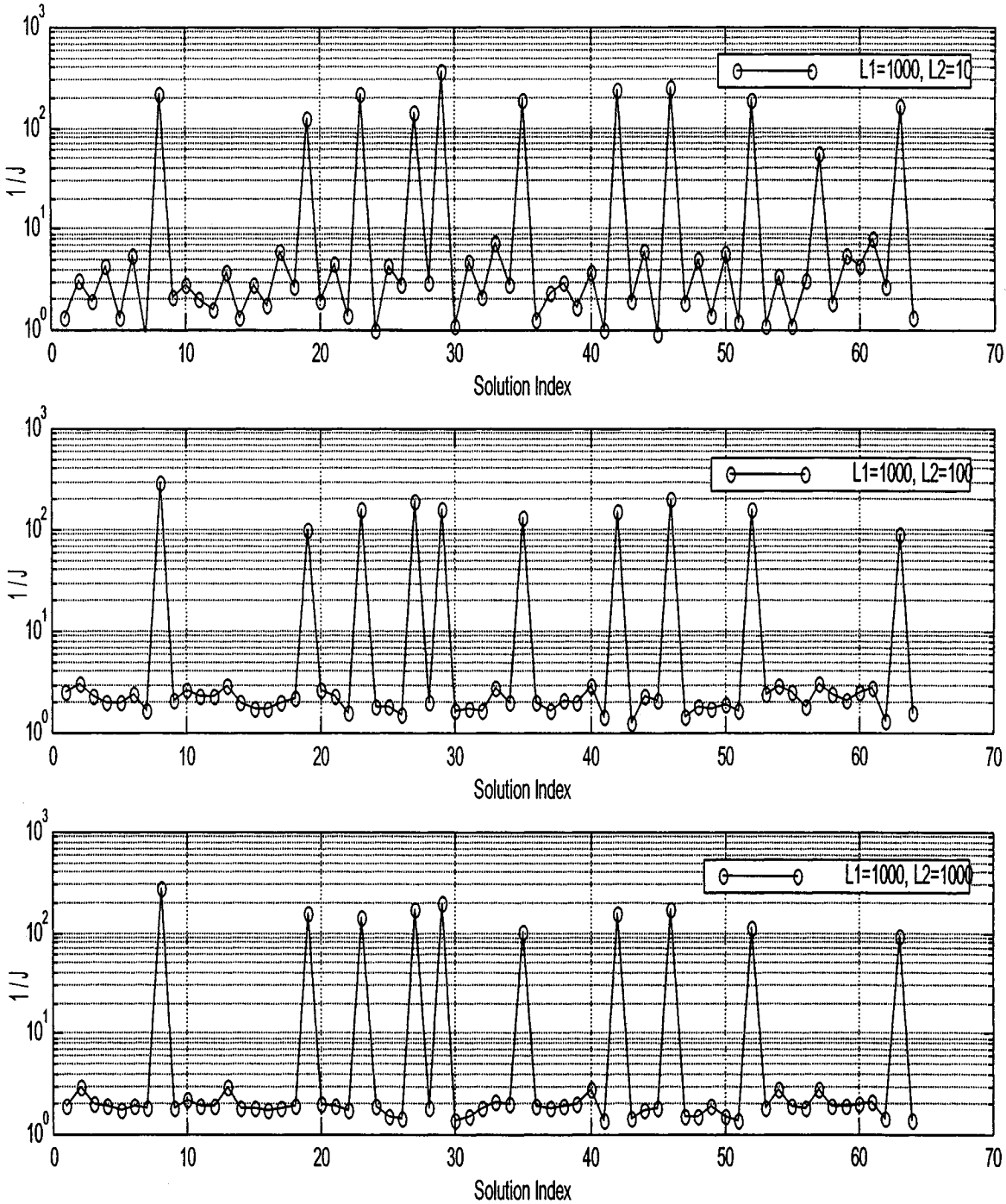


**Figure 4.5 Effect of $L_2$, the accumulation length required for evaluation of the autocorrelation matrix, on the detection process**

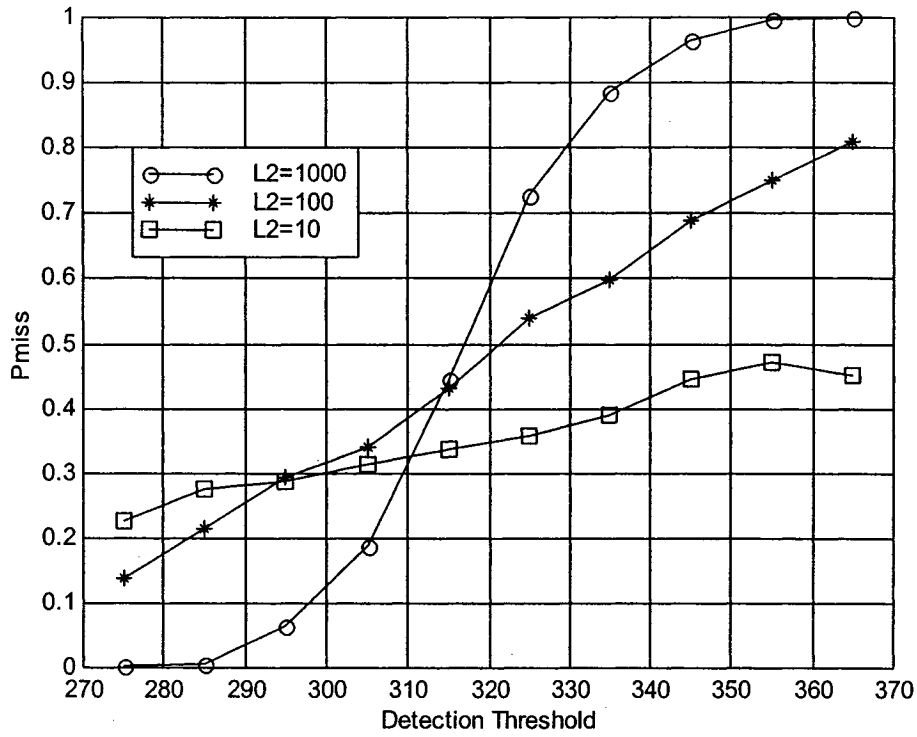


**Figure 4.6 Probability of missed detection for different observation length L2, SNR=25dB**

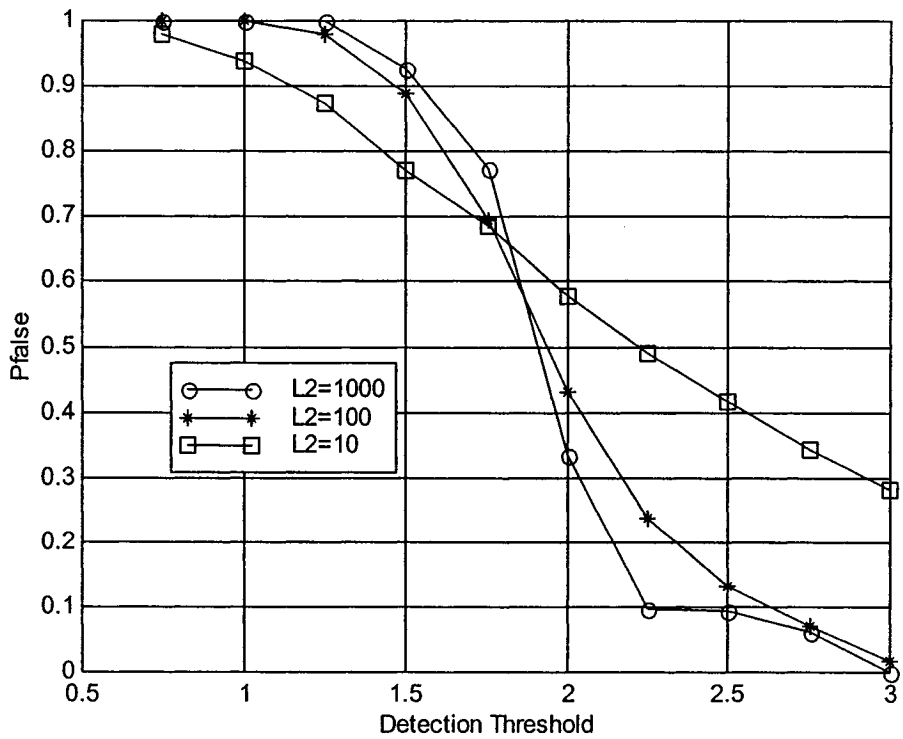


**Figure 4.7 Probability of false detection for different observation length L2, SNR=25dB**

The difference between the two cases can be explained as follows. In order to detect an active user, the cost function associated to it needs to be minimized. Clearly, the minimization becomes more accurate as more statistics becomes available for measurement. However, since for a false solution, there is an inherent factor of dispersion, then the observation length $L_2$ does not need to be very long.

## *4-3.2. Exempting Improper Waveforms from the Search*

By applying a simple constraint on candidate waveforms, we can limit the search over the signal space and significantly reduce the computational load. The source or the logic behind constraints can vary. Spreading waveforms are used for spreading as well as channelization. The main distinction is, when a certain degree of spreading is required not every sequence from the pool of $2^{N-1}$ is appropriate. For example, since the system intends to have a processing gain of $N$, any candidate that does not have a certain number of chip cycle transitions has to be dropped without any further inspection. Figure 4.8 shows the effectiveness of imposing constraints in reducing the number of candidate waveforms. For example, for a processing gain of $N$=16, by having a constraint of 5 chip-cycle transitions, the number of qualified waveforms falls to only %30 of the waveforms. This in turn leads to a similar reduction in the order of complexity.

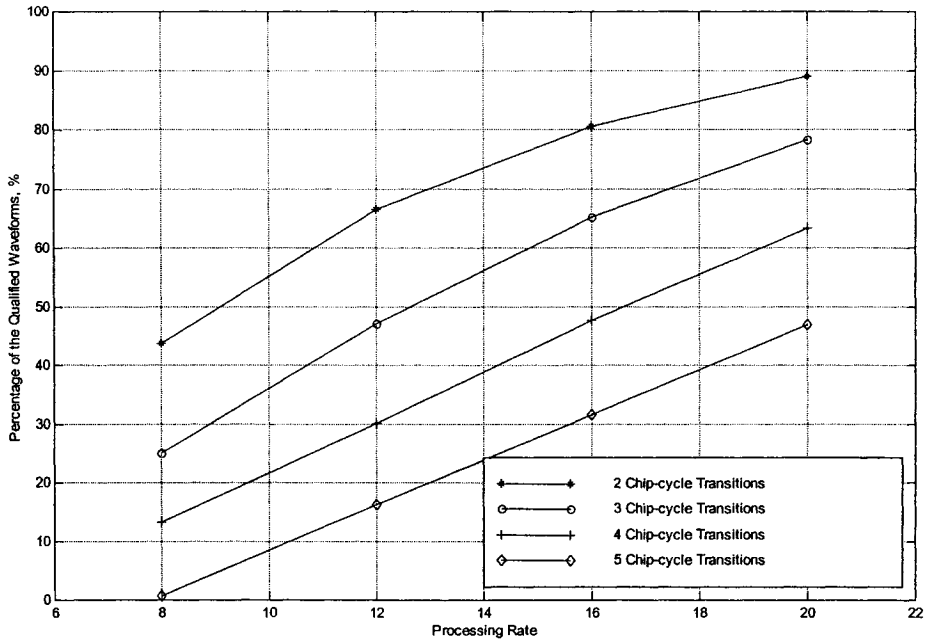


**Figure 4.8 The effect of applying constraints in reducing the search**

## *4-3.3. Efficient Evaluation of C in an Asynchronous System*

In an asynchronous system, new subspace information requires new sample collection to form **C** and to perform EVD on it. Therefore for a system with a spreading factor of $N$, $N$ collections are required. Figure 4.9 shows, the sliding of the collection window for evaluation of **C**. If an arbitrary point for collection of samples is assumed, then the autocorrelation matrix corresponding to that point is referred to as $\mathbf{C}_0$, and the autocorrelation matrix corresponding to a starting point shifted by $kT_c$ is called $\mathbf{C}_k$.. For a system with a processing gain of $N$, all the autocorrelation matrices up to $\mathbf{C}_{N-1}$ have to be evaluated.

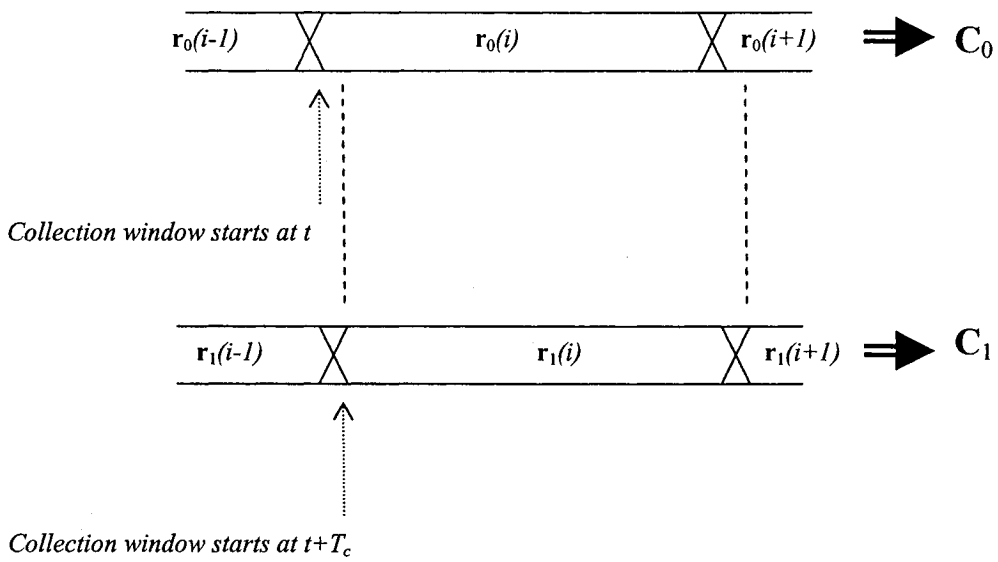


**Figure 4.9 Evaluation of the autocorrelation matrix at different starting points**

When the collection window starts at $t$,

$$\mathbf{C}_0 = E\left\{\mathbf{r}_0(i)\mathbf{r}_0(i)^H\right\} \tag{4.1}$$

and if the collection windows starts at $t+T_c$, we have

$$\mathbf{C}_1 = E\left\{\mathbf{r}_1(i)\mathbf{r}_1(i)^H\right\} \tag{4.2}$$

where $\mathbf{r}_0(i)$ and $\mathbf{r}_1(i)$ represent the received vectors that correspond to the collection starting points $t$ and $t+T_c$. By noting Figure 4.9, $\mathbf{r}_1(i)$ can be written as

$$\begin{aligned}\mathbf{r}_1(i) &= \begin{bmatrix} r_{02}(i) \\ r_{03}(i) \\ \vdots \\ r_{0N}(i) \\ 0 \end{bmatrix} + \begin{bmatrix} 0 \\ 0 \\ \vdots \\ 0 \\ r_{01}(i+1) \end{bmatrix} \\ &= \mathbf{P}_1\mathbf{r}_0(i) + \mathbf{P}_2\mathbf{r}_0(i+1)\end{aligned} \tag{4.3}$$

where $\mathbf{P}_1$ and $\mathbf{P}_2$ are shift-permutation matrices defined as

$$\mathbf{P}_1 = \begin{bmatrix} 0 & 1 & 0 & 0 \\ 0 & 0 & \ddots & 0 \\ 0 & \ddots & \ddots & 1 \\ 0 & 0 & 0 & 0 \end{bmatrix} \tag{4.4}$$

$$\mathbf{P}_2 = \begin{bmatrix} 0 & 0 & 0 & 0 \\ 0 & 0 & \ddots & 0 \\ 0 & \ddots & \ddots & 0 \\ 1 & 0 & 0 & 0 \end{bmatrix} \tag{4.5}$$

Then Equation (4.2) can be rewritten as,

$$\begin{aligned} \mathbf{C}_1 &= E\left\{(\mathbf{P}_1\mathbf{r}_0(i)+\mathbf{P}_2\mathbf{r}_0(i+1))(\mathbf{P}_1\mathbf{r}_0(i)+\mathbf{P}_2\mathbf{r}_0(i+1))^H\right\} \\ &= E\left\{\mathbf{P}_1\mathbf{r}_0(i)\mathbf{r}_0(i)^H\mathbf{P}_1{}^H + \mathbf{P}_1\mathbf{r}_0(i)\mathbf{r}_0(i+1)^H\mathbf{P}_2{}^H\right\}+ \\ &\quad E\left\{\mathbf{P}_2\mathbf{r}_0(i+1)\mathbf{r}_0(i)^H\mathbf{P}_1{}^H + \mathbf{P}_2\mathbf{r}_0(i+1)\mathbf{r}_0(i+1)^H\mathbf{P}_2{}^H\right\} \end{aligned} \tag{4.6}$$

Since the received vector is a statistically independent random sequence, then

$$E\left\{\mathbf{r}_0(i)\mathbf{r}_0(i+1)^H\right\} = 0 \tag{4.7}$$

$$E\left\{\mathbf{r}_0(i+1)\mathbf{r}_0(i)^H\right\} = 0 \tag{4.8}$$

Thus $\mathbf{C}_1$ can be simply evaluated from $\mathbf{C}_0$ as

$$\begin{aligned} \mathbf{C}_1 &= \mathbf{P}_1E\left\{\mathbf{r}_0(i)\mathbf{r}_0(i)^H\right\}\mathbf{P}_1{}^H + \mathbf{P}_2E\left\{\mathbf{r}_0(i+1)\mathbf{r}_0(i+1)^H\right\}\mathbf{P}_2{}^H \\ &= \mathbf{P}_1\mathbf{C}_0\mathbf{P}_1{}^H + \mathbf{P}_2\mathbf{C}_0\mathbf{P}_2{}^H \end{aligned} \tag{4.9}$$

and from there,

$$\mathbf{C}_i = \mathbf{P}_1\mathbf{C}_{i-1}\mathbf{P}_1{}^H + \mathbf{P}_2\mathbf{C}_{i-1}\mathbf{P}_2{}^H \qquad 0 < i < N \tag{4.10}$$

Therefore, in an asynchronous system, it is only required that the autocorrelation matrix be evaluated completely once for an arbitrary starting point. Then from that, the autocorrelation matrices for other starting points can be derived using Equation (4.10).

By employing this method, after the evaluation of $\mathbf{C}_0$ once, the wait time for collection of $L_1$ samples for consequent $\mathbf{C}_i$'s will be saved.

## 4-4. Probabilities of False and Missed Detections

In the calculation of the cost function, measurement errors occur that causes deviations from the nominal values. The result will be declaration of a false solution as an authentic solution and the vice versa.

An important measurement error is due to the limited observation lengths of $L_1$ and $L_2$. Since $L_1$ and $L_2$ are not infinite, $E(z_i^2)$, $E(|z_i|)$ and consequently $J(\mathbf{d}_i)$ will be evaluated with some error. As shown in the previous section, reasonable choices for $L_1$ and $L_2$ are required to reduce the likelihood of detection errors and at the same time to avoid an excessive amount of processing delay. The effect of finite observation length $L_1$, on EVD evaluation has been studied [32]. Therefore, here the focus is only on the measurement errors due to a finite observation length for $L_2$ and its influence on the evaluation of the cost function.

A proper assessment of the performance of the proposed approach is to measure the probability of missed and false detections. A missed detection occurs when the value of $J(\mathbf{d}_i)^{-1}$ resulting from an authentic solution falls below the threshold. Then, the probability of a missed detection can be defined as

$$P_{miss} = p\left(J(\mathbf{d}_i)^{-1} < \eta \,|\, \mathbf{s}_i \text{ is authentic}\right) \tag{4.11}$$

On the other hand, a false detection occurs when $J(\mathbf{d}_i)^{-1}$ resulting from a false solution, exceeds the threshold. Similarly, the probability of a false detection can be defined as

$$P_{false} = p\left(J(\mathbf{d}_i) < \eta^{-1} \,|\, \mathbf{s}_i \text{ is false}\right) \tag{4.12}$$

where $\eta$ is a threshold.

In order to evaluate the above probabilities, the density functions of $J(\mathbf{d}_i)^{-1}$ and $J(\mathbf{d}_i)$ for each case need to be found. However, by employing some approximations, alternative approaches can be utilized to evaluate Equation (4.11) and Equation (4.12).

In practice, for the evaluation of $J(\mathbf{d}_i)$, sample mean-absolute $\overline{|z|}$, and sample variance $\bar{v}$ are used instead of $E(|z_i|)$ and $E(z_i^2)$, where

$$\overline{|z|} = \frac{1}{L_2}\sum_{i=1}^{L_2}|z_i| \tag{4.13}$$

$$\bar{v} = \frac{1}{L_2 - 1}\sum_{i=1}^{L_2}(z_i - \bar{z})^2 \tag{4.14}$$

Since $z_i$'s are uncorrelated, the following can be concluded [33], for $\overline{|z|}$,

$$E\left(\overline{|z|}\right) = E(|z_i|) \tag{4.15}$$

$$\sigma_{\overline{|z|}}^2 = \frac{\sigma_{z_i}^2}{L_2} \tag{4.16}$$

Assuming a large value for $L_2$ and a zero mean Gaussian distribution for $z_i$, then for $\bar{v}$

$$E(\bar{v}) = E(z_i^2) \tag{4.17}$$

$$\sigma_{\bar{v}}^2 = \frac{2\sigma_{z_i}^4}{L_2} \tag{4.18}$$

Since $L_2$ is assumed large, by using the central limit theorem, a Gaussian distribution for $\bar{v}$ and $\overline{|z|}$ can be considered.

## 4-4.1. *Probability of Missed Detection*

If the threshold is set higher than a certain value, then it is probable that some or all of the active users be left un-detected. Therefore, the likelihood of a missed detection for a given threshold needs to be evaluated. For an authentic solution, $J(\mathbf{d}_i)^{-1}$ is evaluated to be,

$$J(\mathbf{d}_i)^{-1} = \left| \frac{E(z_i^{\,2})}{E^2(|z_i|)} - 1 \right|^{-1} = \left| \frac{E(z_i^{\,2}) - E^2(|z_i|)}{E^2(|z_i|)} \right|^{-1} = \left| \frac{A_i^{\,2} + \sigma_{w_i}^{\,2} - A_i^{\,2}}{E^2(|z_i|)} \right|^{-1} = \frac{E^2(|z_i|)}{\sigma_{w_i}^{\,2}} \tag{4.19}$$

Then, the estimate of $J(\mathbf{d}_i)^{-1}$ based on the sample statistics is

$$\tilde{J}(\mathbf{d}_i)^{-1} = \frac{\overline{|z|}^2}{\sigma_{w_i}^{\,2}} \tag{4.20}$$

As explained before, $\overline{|z|}$ can be assumed to have a Gaussian distribution with the parameters stated in Equation (4.15) and Equation (4.16). Then, $\tilde{J}(\mathbf{d}_i)^{-\frac{1}{2}}$ will also have a Gaussian distribution with the following features

$$m_{\tilde{J}^{-\frac{1}{2}}} = \frac{E(|z_i|)}{\sigma_{w_i}} = \frac{A_i}{\sigma_{w_i}} \tag{4.21}$$

$$\sigma^2_{\tilde{J}^{-\frac{1}{2}}} = \frac{E(z_i^{\,2})}{L_2 \sigma^2_{w_i}} = \frac{1}{L_2}\left(1 + \frac{A_i^{\,2}}{\sigma^2_{w_i}}\right) \tag{4.22}$$

Thus, $\tilde{J}(\mathbf{d}_i)^{-1}$, that is actually the square of $\tilde{J}(\mathbf{d}_i)^{-\frac{1}{2}}$, has a density function described by the following [33]

$$f_{\tilde{J}^{-1}}(\psi)=\begin{cases}\dfrac{1}{2\sqrt{2\pi\psi}\sigma_{\tilde{J}^{-\frac{1}{2}}}}\left(\exp\left\{-\dfrac{\left(\sqrt{\psi}-m_{\tilde{J}^{-\frac{1}{2}}}\right)^2}{2\sigma_{\tilde{J}^{-\frac{1}{2}}}^2}\right\}+\exp\left\{-\dfrac{\left(\sqrt{\psi}+m_{\tilde{J}^{-\frac{1}{2}}}\right)^2}{2\sigma_{\tilde{J}^{-\frac{1}{2}}}^2}\right\}\right) & \psi>0\\ 0 & \psi<0\end{cases} \tag{4.23}$$

Therefore, the probability of error can be evaluated by integrating Equation (4.23) over the relevant range

$$P_{miss}=\int_0^{\eta} f_{\tilde{J}^{-1}}(\psi)dJ\psi \tag{4.24}$$

## *4-4.2. Probability of False Detection*

A comparison between Equations (4.16) and (4.18) reveals that the measurement error of $E(z_i^{\,2})$ is significantly greater than the measurement error of $E^2(|z_i|)$.

$$\frac{\sqrt{2}\sigma_{z_i}^{\,2}}{\sqrt{L_2}} >> \frac{\sigma_{z_i}^{\,2}}{L_2} \tag{4.25}$$

This would not have much impact for the case of an authentic solution. Because, in terms of the percentage of the measured parameter; i.e., $\dfrac{\sigma_{\bar{v}}^{\,2}}{E(z_i^{\,2})}$ or $\dfrac{\sigma_{|\bar{z}|}^{\,2}}{E^2(|z_i|)}$, the error is negligible. However, in the case of a false solution that is of interest in evaluation of false detection. Then as expressed in (2.25), $\sigma_{\bar{v}}^{\,2}$ is the dominant source of the error. Therefore, for simplicity we can ignore the measurement error in $E(|z_i|)$ and merely focus on the

error contribution from $\bar{v}$. Since $L_2$ is large, using the central limit theorem, a Gaussian distribution for $\bar{v}$ can be considered as

$$f_{\bar{v}}(\bar{v}) = \frac{1}{\sqrt{2\pi}\sigma_{\bar{v}}} \exp\left( \frac{-\left(\bar{v} - E\left(z_i^{\,2}\right)\right)^2}{2\sigma_{\bar{v}}^{\,2}} \right) \tag{4.26}$$

Then, the distribution of

$$\tilde{J}(\mathbf{d}_i) = \left( \frac{\bar{v}}{E^2(|z_i|)} - 1 \right) \tag{4.27}$$

will be Gaussian as well, with the following parameters

$$m_{\tilde{J}} = \left( \frac{E\left(z_i^{\,2}\right)}{E^2(|z_i|)} - 1 \right) = \frac{\pi - 2}{2} \tag{4.28}$$

$$\sigma_{\tilde{J}} = \sqrt{\frac{2}{L_2}} \frac{\sigma_{z_i}^{\,2}}{E^2(|z_i|)} = \frac{\pi}{\sqrt{2L_2}} \tag{4.29}$$

Using the above derivations, Equations (4.11) and (4.12) can be evaluated as

$$\begin{aligned} P_{false} &= p\left(J(\mathbf{d}_i) < \eta^{-1} \,|\, \mathbf{s}_i \text{ is false}\right) \\ &= \frac{1}{\left(\pi\sqrt{\frac{\pi}{L_2}}\right)} \int_{-\infty}^{\eta^{-1}} \exp\left( \frac{-\left(x - \left(\frac{\pi - 2}{2}\right)\right)^2}{\left(\frac{\pi^2}{L_2}\right)} \right) dx \end{aligned} \tag{4.30}$$

***Some observations:***

- As expected, increasing the observation length $L_2$, improves the accuracy of the estimation.
- The parameters for an authentic solution are functions of the signal to noise ratio of the active user. A higher signal-to-noise ratio leads to lower variance in the evaluation of $\tilde{J}(\mathbf{d}_i)$.

- For the case of a false solution, the accuracy of the estimation depends only on the observation length $L_2$.

Figure 4.10 and Figure 4.11 show the simulation versus the analytical results for missed and false detections. The processing gain is $N$=16, $L_1$=10000 and $L_2$=250. In both Figures, the probability of missed detections is plotted versus the threshold $\eta$. Figure 4.10 shows the probability of missed detection for a user with a SNR of 15 dB. Figure 4.11 exhibits the probability of false detection in a model where there are 10 equal power active users each with a SNR of 15 dB. In both cases, presented in Figure 4.10 and Figure 4.11, simulation and analytical results are in close agreement.

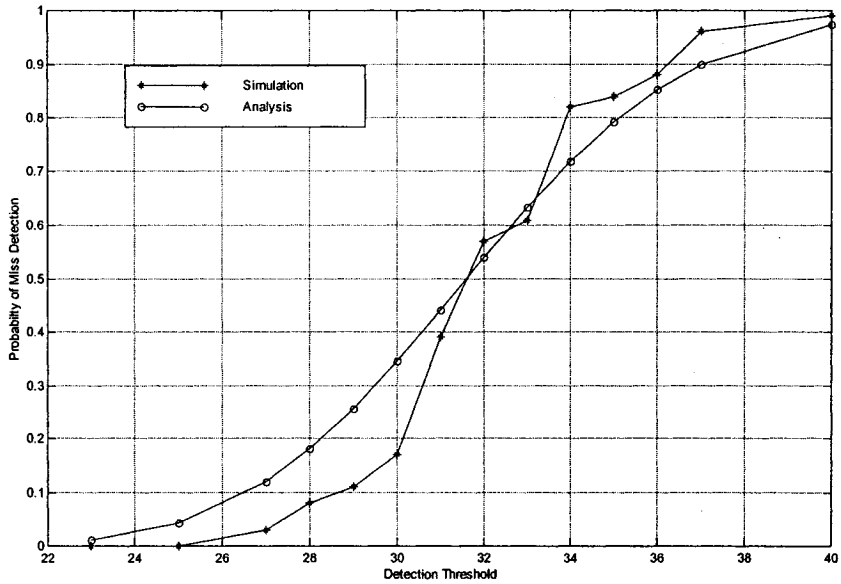


**Figure 4.10 Simulation and analytical results for probability of missed detection**

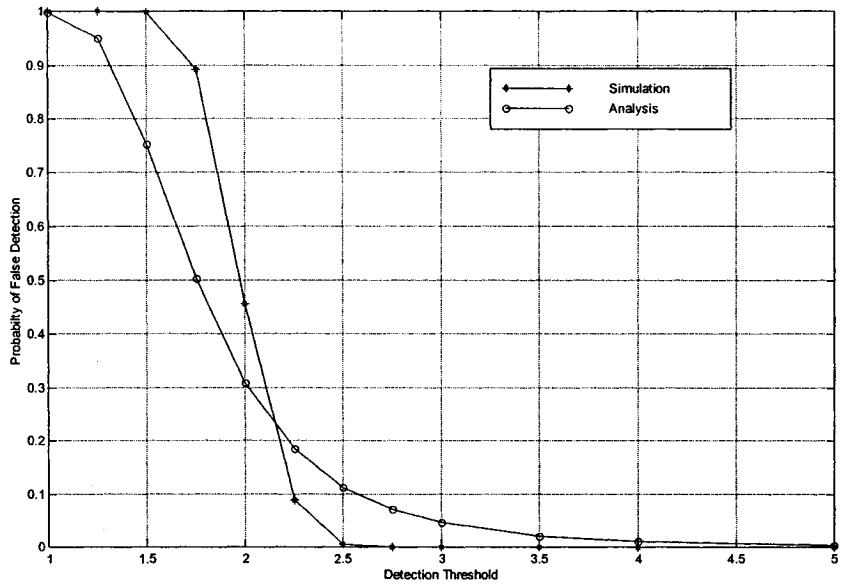


**Figure 4.11 Simulation and analytical results for probability of false detection**

## *4-4.3. Performance in AWGN and Rayleigh Fading Channels*

Figure 4.12 shows probabilities of false and missed detections in an AWGN channel at different SNR's. In each case, the detection test is repeated 100 times and then the number of errors is averaged. As Figure 4.12 shows, the number of false detections reduces while the number of missed detections mounts as the threshold is increased. If the impact of a missed detection is equal to a false detection, then the optimum threshold for each case is the threshold value corresponding to the cross over point or region of the two graphs. For high SNR's, the range of proper threshold values becomes wider. However, at low SNR's, the selection of the threshold is significantly more delicate.

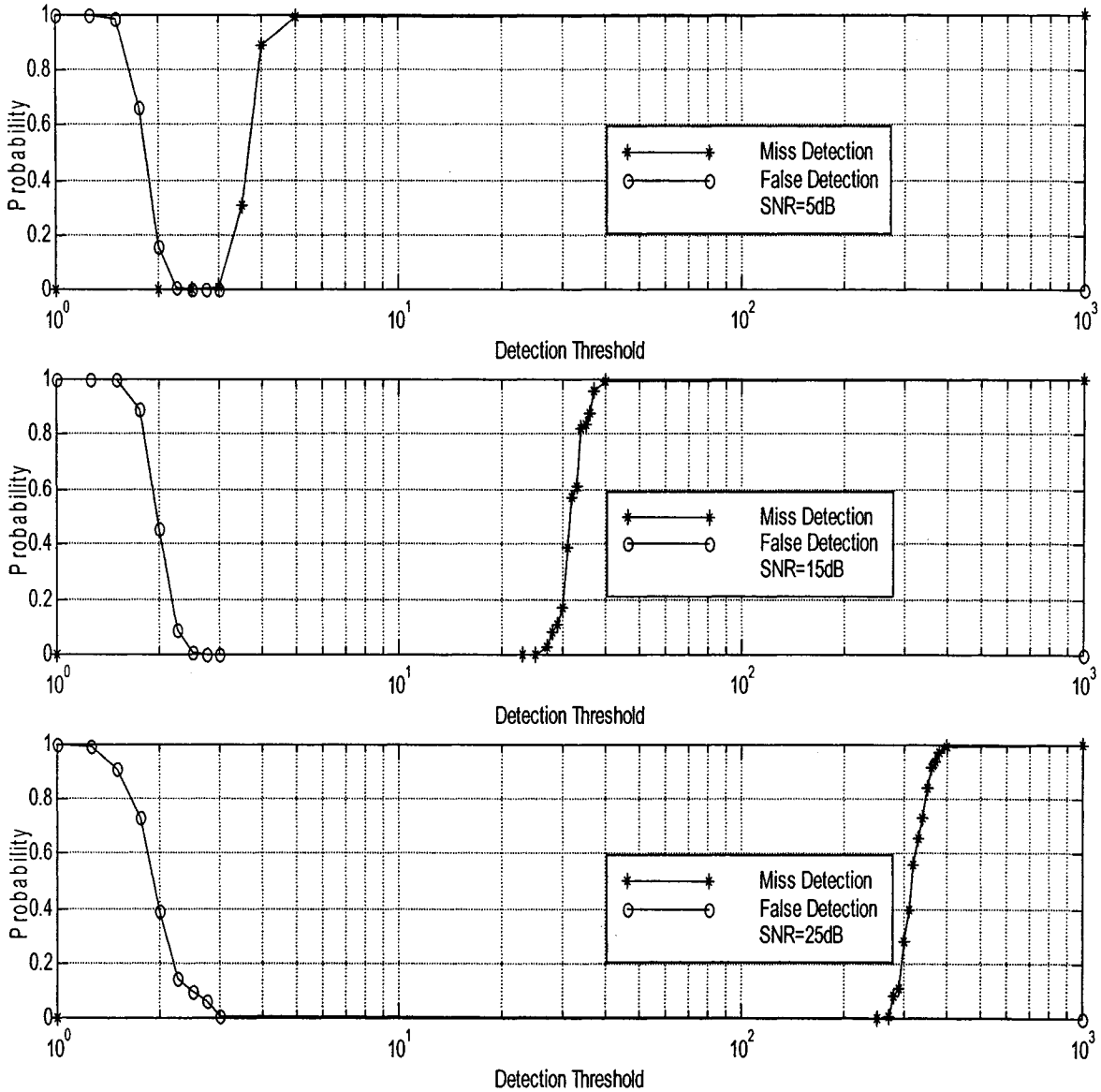


**Figure 4.12 Simulation results for probability of false and missed detections in Gaussian channel**

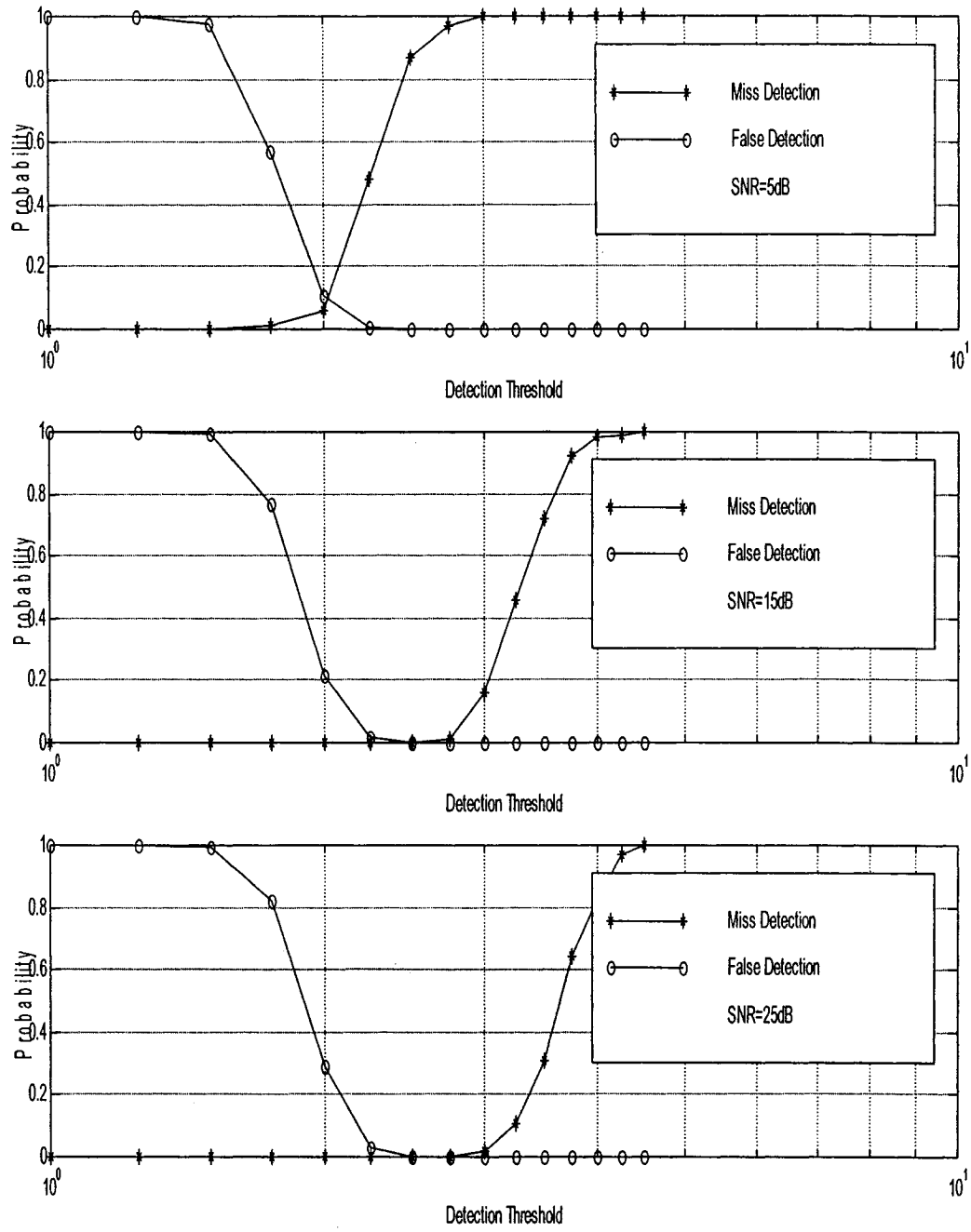


**Figure 4.13 Simulation results for probability of false and missed detections in a Rayleigh channel**

Figure 4.13 shows the simulation results for a Rayleigh fading channel. For such a model, following observations can be made. First, the general behavior of the probability of false detection is not different from a Gaussian channel and also is not much affected by SNR of the active users. This can be justified by noting that when the number of active users, $K$, is large the approximation of $z_i$ in Equation (3-40), to a Gaussian distribution is not influenced by either amplitude or SNR variations of the active users. On the other hand, the probability of miss detection is considerably deteriorated by the existence of fading in the channel. This necessitates a refined selection for the threshold to minimize detection errors.

## *4-4.4. Selection of the Detection Threshold*

As exhibited in (3-39), the value of the inverse cost function for an authentic solution is

$$\frac{1}{J(\mathbf{d}_i)} = \frac{A_i^{\,2}}{\sigma_{w_i}^{\,2}} = \frac{A_i^{\,2}}{(\mathbf{d}_i^T \mathbf{d}_i)\sigma^2} \propto \mathrm{SNR}_i \qquad \textbf{(4. 31)}$$

where $\mathrm{SNR}_i$ represents the signal to noise ratio of the $i_{\mathrm{th}}$ active user. Thus, the cost function approaches zero as the signal to noise ratio increases. On the other hand, for a false solution

$$J(\mathbf{d}_i) = \left| \frac{E\left(z_i^{\,2}\right)}{E^2\left(|z_i|\right)} - 1 \right| = \left| \frac{\sigma_{z_i}^{\,2}}{\frac{2}{\pi}\sigma_{z_i}^{\,2}} - 1 \right| = \frac{\pi - 2}{2}. \qquad \textbf{(4. 32)}$$

If we equate Equation (4.31) with Equation (4.32), a minimum approximate value for the $\mathrm{SNR}_i$ required for detection becomes available

$$\mathrm{SNR}_{i\min} = \frac{2}{\pi - 2} \approx 1.75 \equiv 2.4\,\mathrm{dB} \tag{4.33}$$

Thus, in an AWGN channel, an active user must have a SNR of more than 2.4 dB in order to be detected. Thus, the threshold $\eta$ should be selected in such a way to have a reasonable margin from Equation (4.32) while being not too high to cause miss detection of the active users. For example, if the minimum expected SNR of an active user in a cell is 10dB, then the threshold can be selected in the range of,

$$1.75 \le \eta \le 10 \tag{4.34}$$

Although, this is not an accurate approach for setting the threshold, it could be very helpful to appreciate its range. Also it is worth mentioning that the presented simulation results in Figures 4.12 and 4.13 confirm this finding.

## *4-5. Improved Estimation of User's Timing*

In the basic model presented in the Chapter 3, the sampling interval is assumed $T_c$ or a chip interval. Therefore, the capability of resolving timing of the users is limited to a chip period. However in an over-sampled system, the received signal is sampled at a rate of higher than the chip rate. Thus, a higher resolution in timing estimation can be expected and users' timing can be estimated more precisely. The implication of such consideration is that the dimension of the receive vector and consequently the autocorrelation matrix and all other related vectors increase. This increase in dimension makes the computational burden more prominent.

Figures 4.14-4.17 show simulation result for timing estimation and user identification in an asynchronous system with $N$=8. The over-sampling is assumed to be 2. Therefore,

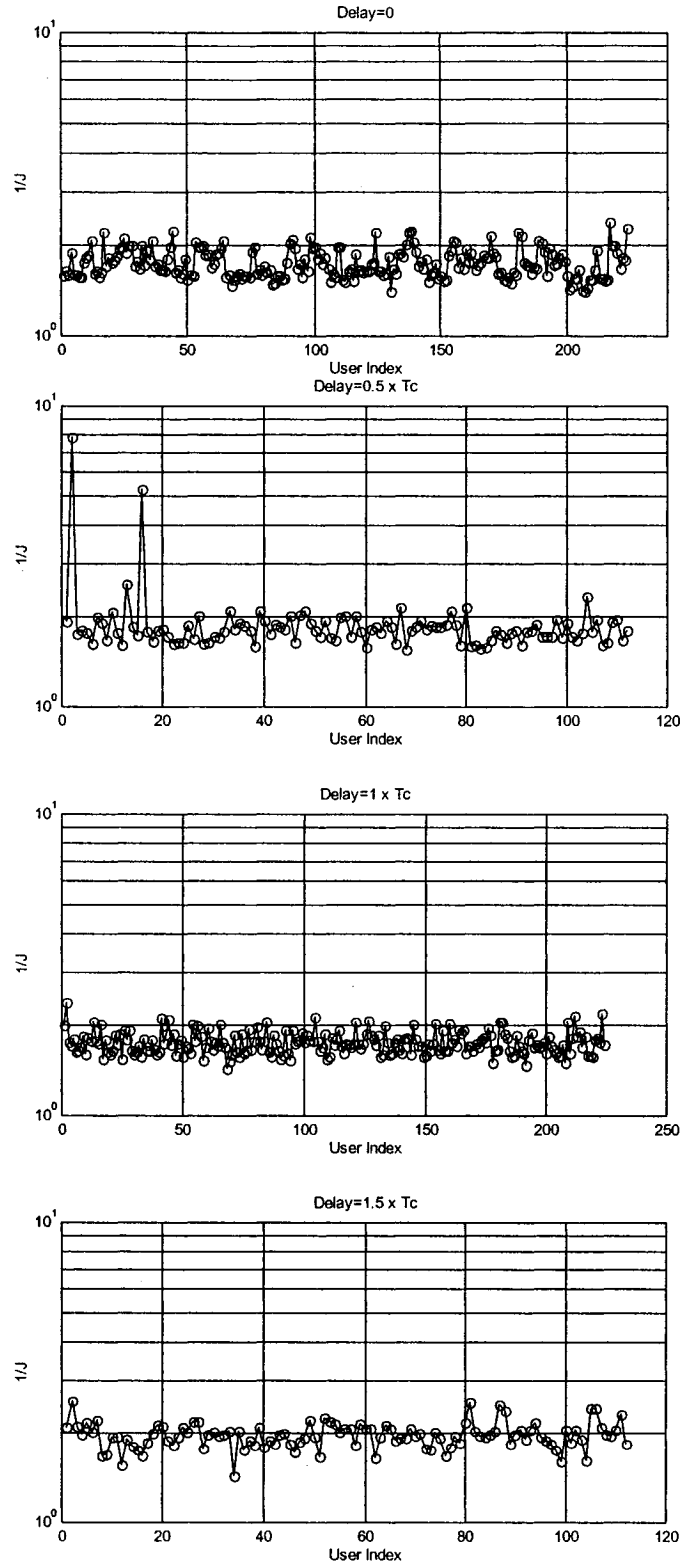


**Figure 4.14 Timing search in an over-sampled model for 0 to 1.5$T_c$**

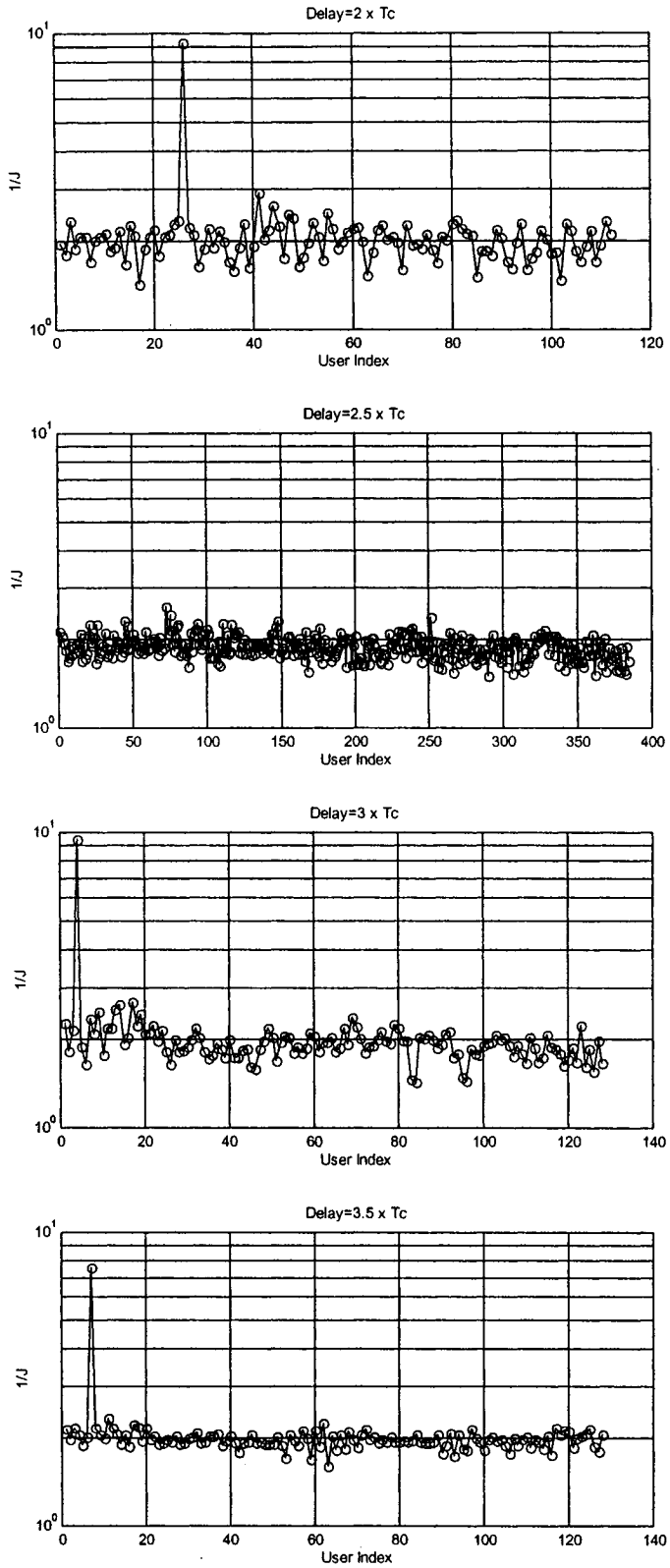


**Figure 4.15 Timing search in an over-sampled model for $2T_c$ to $3.5T_c$**

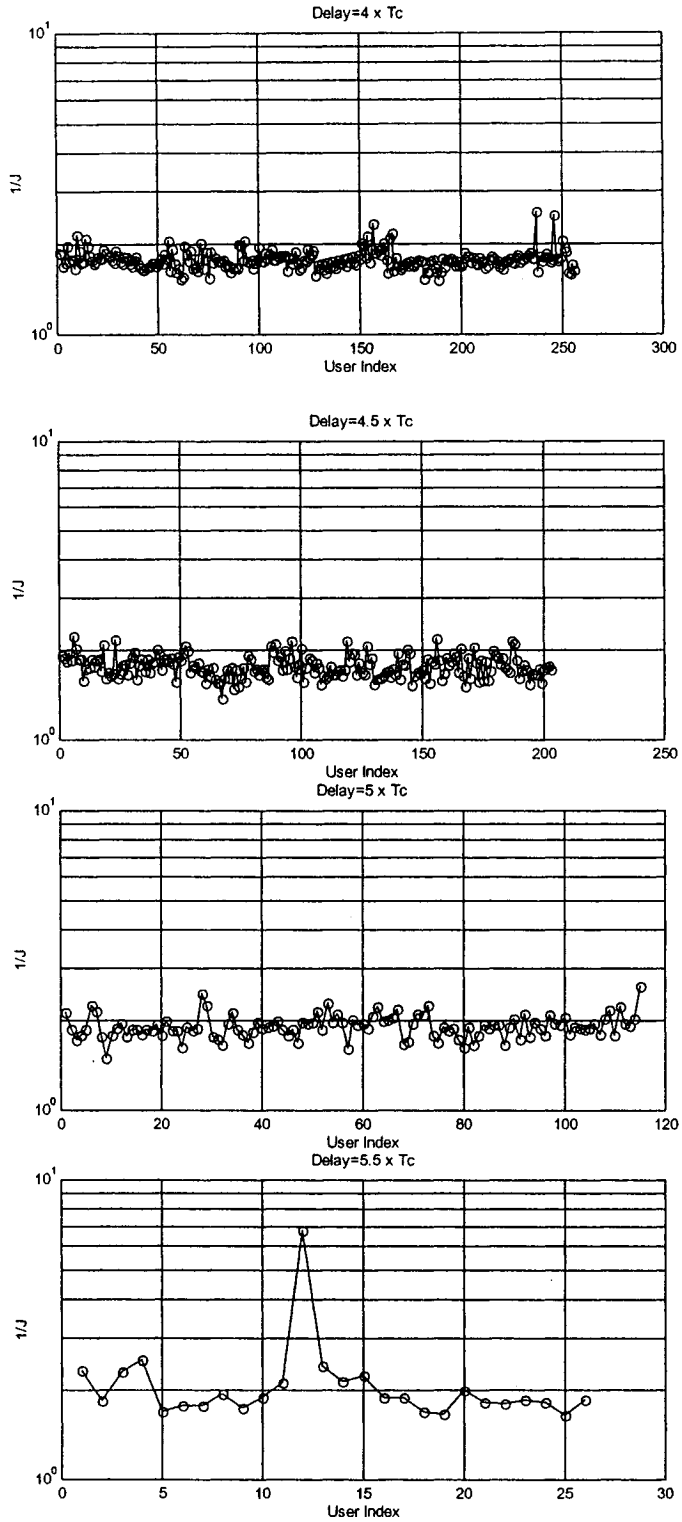


**Figure 4.16 Timing search in an over-sampled model for $4T_c$ to $5.5T_c$**

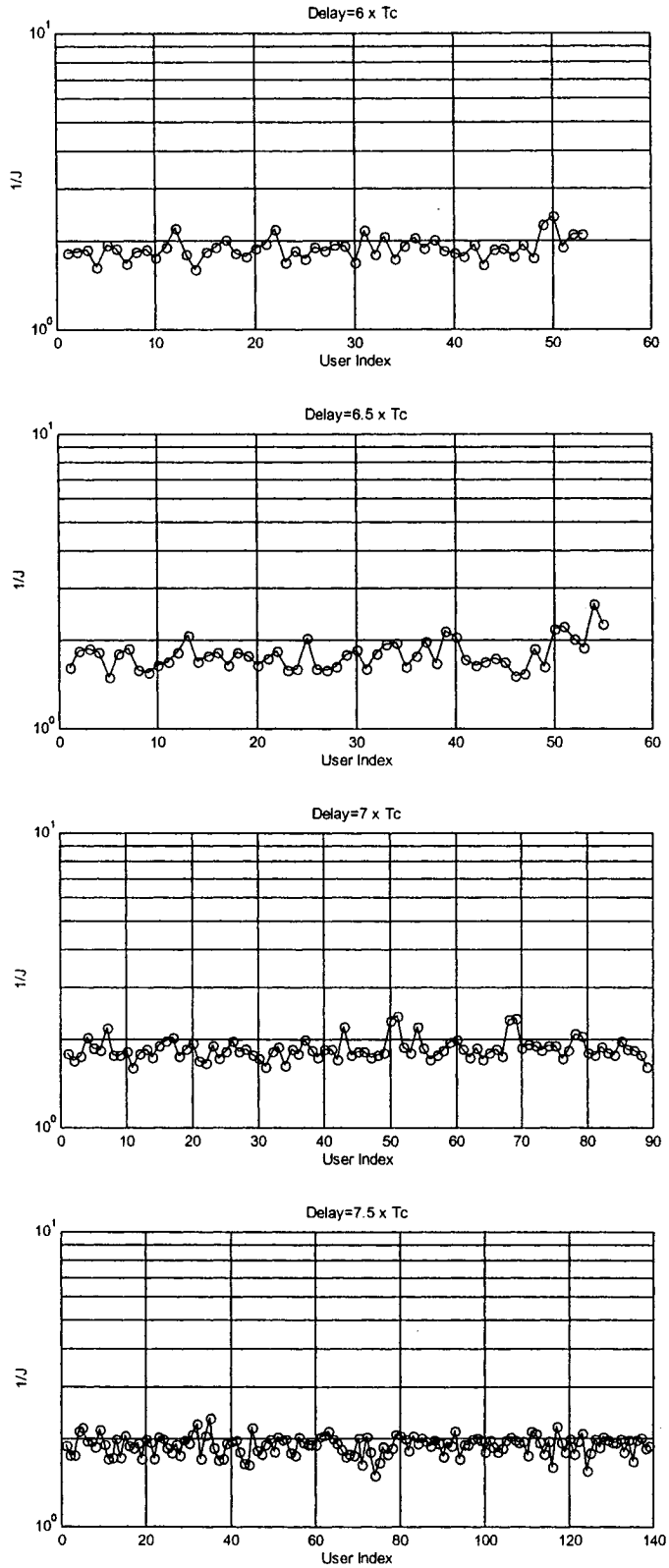


**Figure 4.17 Timing search in an over-sampled model for $4T_c$ to $7.5T_c$**

the dimension of the receive vector and the correlation matrix are "16 x 1" and "16 x 16", respectively. It is also assumed that there are six active users in the system with different delays. Since the processing gain is $N$=8, there are 16 snap shots. Each snapshot shows the results of signal projection and cost function evaluation for that particular value of the delay. For each snapshot, Equation (3.33) is evaluated. The term "Delay" in the Figures (4.14)–(4.17) describes the timing relation of the collection window with respect to the active users. In the simulation, users are assumed to have the following delays with respect to the initial start point of the collection window:

$$\text{User } 1 \rightarrow 0.5T_c,$$
$$\text{User } 2 \rightarrow 0.5T_c,$$
$$\text{User } 3 \rightarrow T_c,$$
$$\text{User } 4 \rightarrow 3T_c,$$
$$\text{User } 5 \rightarrow 3.5T_c,$$
$$\text{User } 6 \rightarrow 5.5T_c.$$

Then for example, in Figure 4.14, the graph for "*Delay*=$0.5T_c$" shows two peaks that indicate that there are two synchronous users operating in the system with a relative delay of $0.5T_c$ with respect to the initial starting point of the collection window. Also, snapshots with no peak present imply that there are no active users operating with this timing.

## *4-6. Conclusion*

In this chapter the performance of our proposed algorithm is investigated. It is shown that the algorithm exhibits a consistent behavior over several trials. Also, it is shown that by applying a simple restriction on the spreading code candidates, the search can be significantly speeded up and the algorithm can be made more agile. Moreover, an

efficient method for evaluation of autocorrelation matrix in asynchronous systems is presented. The performance of the detector is investigated by evaluating the probability of the false alarm and miss detections. A fading channel causes significant degradation on the probability of miss detection while does not affect much the probability of false detection. It was also shown that by over-sampling the receive signal, the timing estimation of active users can be performed with more precision.

# *Chapter 5*

# *Conclusion*

## *5-1. Conclusion and Summary*

CDMA-based systems are widely used in various wireless applications. In order to exploit the capacity of a CDMA system, multiuser detection techniques are essential. In any multiuser detection scheme, some prior knowledge of the user parameters, e.g., the spreading code, timing, and power is assumed. However, in a real system, this may not be the case. Users enter and exit the system irregularly and the base station has to continuously keep track of the status of each user.

Various methods could be used to transfer users' parameters to the base station, however, one way or the other, they impose some overhead and reduce system efficiency. Therefore, another important aspect of the CDMA reception is to assist multiuser

detection schemes by user identification. This enables the receiver to dynamically adapt itself to the multiuser environment.

Several user identification schemes are introduced [18]-[27]. In all of these schemes, the prior knowledge of the signature sequences or some other form of constraint on the system is assumed, i.e., training sequences or direction of reception. The main contribution of this thesis is that the proposed approach does not require the prior knowledge of the signature sequences nor does it rely on other conditions or requirements called for in the previous works.

## *5-2. Contribution of the Thesis*

In this work, a blind scheme based on Multiple Signal Classification (MUSIC) algorithm for user identification in a chip-synchronous multiuser CDMA system is suggested. The scheme is blind in the sense that it does not require prior knowledge of the spreading codes. Spreading codes and users' power are acquired by the scheme. Eigenvalue Decomposition (EVD) is performed on the received signal, and then all the valid possible signature sequences are projected onto the subspaces. However, as a result of this process, some false solutions are also produced and the ambiguity seems un-resolvable. Our approach is to apply a transformation derived from the results of the subspace decomposition on the received signal and then to inspect their statistics. Then, the scheme searches over both signal subspace and time domain to minimize a defined cost function.

The proposed scheme is able to perform user identification without any external assistance in both symbol-synchronous and symbol-asynchronous CDMA system. By

employing the proposed scheme, there is no need to any training signal or any constraint on the operation of the system. Published papers based on the results of this work are cited in the reference section of the thesis [35]-[40].

## *5-3. Further Works*

The presented work while solves one particular problem, paves the way towards many more questions as well as other applications. Some of them can be summarized as follows:

- In a symbol-asynchronous system, the proposed method calls for $N$ times EVD and $N*2^{n-1}$ projections. Although, it is shown that by employing simple constraints, the number of projections can be reduced significantly, the whole algorithm remains computation intensive. In order to make the algorithm practical for systems with fast dynamics, less complexity is essential.

- In this work, a decorrelator transformation was devised based on the available subspace information. This choice was based on the fact that by decorrelation can separate users with zero MAI. However, this leads to noise enhancement and causes performance degradation in low signal to noise ratio scenarios. Another alternative to the decorrelator would be MMSE detector. So, the whole method could be repeated by employing the MMSE detection instead of decorrelator.

- In order to distinguish the difference between the statistics of false and authentic solutions, a cost function is defined. This cost function exhibits a feature that shows no reliance on the amplitude information of the signal. In other words, it measures the dispersion of $z_i$, by comparing the two statistics of $z_i$. Therefore, any scalar gain becomes irrelevant. This feature could be used in blind equalization. In existing blind equalization methods such as Constant Modulus Algorithm (CMA), it is assumed that among all the loops in a receiver, at least the Automatic Gain Control (AGC) loop has converged. Therefore the signal at the input of the equalizer is at the nominal level required for the processing. Since the proposed cost function, is independent of the amplitude information, the equalizer is able to converge faster. Similar discussion for the equalizer can be applied for antenna array and beam-forming systems.

# *References*

[1] Wiliam C. Y. Lee, "Overview of Cellular CDMA", *IEEE Transaction on Vehicular Technology*, Volume. 40, No. 2, pp. 291-302, May 1991.

[2] Hikmat Sari, Frederik Vanhaverbeke and Marc Moeneclaey, "Extending the capacity of multiple access channels", *IEEE Communications Magazine*, Volume 38, Issue 1, pp. 74-82, January 2000.

[3] Qulacomm Inc., "An overview of the application of code division multiple access (CDMA) to digital cellular systems and personal cellular networks", Technical Report, May 21, 1992.

[4] Raymond L. Pikholtz, Laurence B. Milstein and Donald L. Schilling, "Spread spectrum for mobile communications", *IEEE Transaction on Vehicular Technology*, Volume. 40, No. 2, pp. 313-321, May 1991.

[5] Andrew J. Viterbi, *CDMA Principles of Spread Spectrum Communication*, Addison-Wesley Wireless Communications Series 1995.

[6] Ramjee Prasad, Tero Ojanpera, "An Overview of CDMA Evolution toward Wideband CDMA", *IEEE Communications Surveys*, 4th Quarter 1998.

[7] Alexandra Duel-Hallen, Jack Holtzman and Zoran Zvonar, "Multiuser detection for CDMA systems", *IEEE Personal Communications Magazine*, Volume 2, Issue 2, pp. 46-58, April 1995.

[8] Shimon Moshavi, "Multiuser Detection for DS-CDMA Communications", *IEEE Communications Magazine*, pp. 124-136, October 1996.

[9] Graeme Woodward and Branka S. Vucetic, "Adaptive Detection for DS-CDMA", *Proceedings of the IEEE*, Volume 86, No. 7, pp. 1413-1434, July 1998.

[10] Michael Honig and Michail K. Tsatsanis, "Adaptive Techniques for Multiuser CDMA Receiver", *IEEE Signal Processing Magazine*, Volume 17, Issue 3, pp. 49-61, May 2000.

[11] Verdu, *Multiuser Detection*, Cambridge University Press, 1st Edition, 1998.

[12] R. Lupas and S. Verdu, "Linear Multiuser Detectors for Synchronous Code-Divisioned Multiple-Access Channel", *IEEE Transaction on Information Theory*, Volume. 35, No. 1, pp. 123-136, Jan. 1989.

[13] Z. Xie, R. T. Short and C.K. Rushfort, "A Family of Suboptimum Detectors for Coherent Multiuser Communications", *IEEE Journal on Selected Areas in Communications*, Volume. 8, No. 4, pp. 683-690, May 1990.

[14] Duel-Hallen, "Decorrelating Decision-Feedback Multiuser Detector for Synchronous Code-Division Multiple-Access Channel", *IEEE Transaction on Communications*, Volume. 41, No. 2, pp. 285-290, February 1993.

[15] P. Patel and J. Holtzman, "Analysis of a Simple Successive Interference Cancellation Scheme in DS/CDMA", *IEEE Journal on Selected Areas in Communications*, Volume. 12, No. 5, pp. 796-807, June 1994.

[16] M.K. Varanasi and B. Aazhang, "Multistage Detection in Asynchronous Code Division Multiple-Access Communications", *IEEE Transaction on Communications*, Volume. 38, No. 4, pp. 509-519, April 1990.

[17] Dariush Divsalar, Marvin K. Simon, Dan Raphaeli, "Improved Parallel Interference Cancellation for CDMA", *IEEE Transaction on Communications*, Volume. 46, No. 2, pp. 258-268, February 1998.

[18] Darryl Deux Lin and Teng Joon Lim, "Subspace-Based Active User Identification for a Collision-Free Slotted Ad Hoc Network", *IEEE Transactions on Communications*, Volume. 52, No. 4, pp. 612-621, April 2004.

[19] Cha'o-Ming Chang and Kwang-Cheng Chen, "Joint Linear User Identification, Timing, Phase, and Amplitude Estimation in DS/CDMA Communications", *IEEE Communications Letters*, Volume. 4, No. 4, pp. 113-115, April 2000.

[20] Xiang Yu and Xian-Da Zhang, "A New Blind Identification Method for DS-CDMA Systems with Antenna Array Under Multipath Fading", *IEEE Journal on*

*Selected Areas in Telecommunications*, Volume. 17, No. 12, pp. 2154-2161, December 1999.

[21] Karen W. Halford and Maite Brandt-Pearce, "New-User Identification in a CDMA System", *IEEE Transactions on Communications*, Volume. 46, No. 1, pp. 144-155, January 1998.

[22] Hui Liu and Guanghan Xu, "A Subspace Method for Signature Waveform Estimation in Synchronous CDMA System", *IEEE Transactions on Communications*, Volume. 44, No. 10, pp. 1346-1354, October 1996.

[23] Thomas Ostman, Stefan Parkvall and Bjorn Ottersten, "An Improved MUSIC Algorithm for Estimation of Time Delays in Asynchronous DS-CDMA Systems", *IEEE Transactions on Communications*, Volume. 47, No. 11, pp. 1628-1633, November 1999.

[24] Yanrong Zhang, Guoan Bi, Boon Poh Ng and A. C. Kot, "A Subspace Method for Signature Waveform Estimation and Detection in Dispersive CDMA Channel", *EUROCOM 2000*, Munich, Germany.

[25] Wei-Chiang Wu, Kwang-Cheng Chen, "Identification of Active Users in Synchronous CDMA Multiuser Detection", *IEEE Journal on Selected Areas in Communications*, Volume. 16, No. 9, pp. 1723-1735, December 1998.

[26] Zhengyuan Xu, "Blind Identification of Co-Existing Synchronous and Asynchronous Users for CDMA Systems", *IEEE Signal Processing Letters*, Volume. 8, No. 7, pp. 212-214, July 2001.

[27] Wei-Chiang Wu and Kwang-Cheng Chen, "Root-MUSIC Based Joint Identification and Timing Estimation of Asynchronous CDMA System over Rayleigh

Fading Channel", *IEICE Transactions on Fundamentals*, Volume. E81-A, No. 8, pp. 1550-1559, August 1998.

[28] Xiaodong Wang and H. Vincent Poor, "Blind Multiuser Detection: A Subspace Approach", *IEEE Transactions on Information Theory*, Volume. 44, No. 2, pp. 677-690, March 1998.

[29] Eric Moulines, Pierre Duhamel, Jean-Francois Cardoso and Sylvie Mayrague, "Subspace Methods for the Blind Identification of Multichannel FIR filters", *IEEE Transaction on Signal Processing*, Volume. 43, No. 2, pp. 516-525, February 1995.

[30] Sumit Roy, "Subspace Blind Adaptive Detection for Multiuser CDMA", *IEEE Transactions on Communications*, Volume. 48, No. 1, pp. 169-175, January 2000.

[31] Erik G. Strom, Stefan Parkvall, Scott L. Miller and Bjorn E. Ottersten, "Propagation Delay Estimation in Asynchronous Direct-Sequence Code-Division Multiple Access Systems", *IEEE Transactions on Communications*, Volume. 44, No. 1, pp. 84-93, January 1996.

[32] P. Stoica and A. Nehorai, "Statistical Efficiency study of Direction Estimation Methods Part I: Analysis of MUSIC and Preliminary Study of MLM", *Advances in Spectrum Analysis and Array Processing Volume. II*, S. Haykin Ed. Englewood Cliffs, NJ: Prentics Hall, 1991, pp. 263-305.

[33] Athanasios Papoulis, "*Probability, Random Variables, and Stochastic Processes*", 3rd Edition, McGraw-Hill 1991.

[34] M.D. Srinath, P.K. Rajsekaran and R. Viswanathan, "*An Introduction to Statistical Signal Processing with Applications*", 1st Edition, Prentice-Hall Inc. 1996.

[35] Afshin Haghigat, M. Reza Soleymani, "A MUSIC-based algorithm for blind user identification in multiuser DS-CDMA", *EURASIP Journal on Applied Signal Processing, Special Issue on Improved CDMA Detection Techniques for Future Wireless Systems*, Spring 2005.

[36] Afshin Haghigat, M. Reza Soleymani, "Joint Detection of Timing and Identity of Users in a Chip-Synchronous Multiuser CDMA System", *IEEE Semiannual Vehicular Technology Conference, VTC2004-Fall*, Los Angeles, CA, Sept.26-29, 2004.

[37] Afshin Haghigat, M. Reza Soleymani, "A Blind MUSIC-based algorithm for User Identification and Power Estimation in Multiuser DS-CDMA", *IEEE 2003 Global Communications Conference*, San Francisco, CA, USA, December 1-5, 2003.

[38] Afshin Haghigat, M. Reza Soleymani, "Blind Spreading Sequence Discovery for DS-CDMA Signal Interception", *Military Communications Conference 2003, MILCOM 2003*, Boston, MA, USA, October 13-16, 2003.

[39] Afshin Haghigat, M. Reza Soleymani, "A MUSIC-based algorithm for Spreading Sequence Discovery in Multiuser DS-CDMA", *IEEE Semiannual Vehicular Technology Conference, VTC-Fall 2003*, Orlando, Florida, USA October 6-9, 2003.

[40] Afshin Haghigat, M. Reza Soleymani, "A Subspace Scheme for Blind User Identification in Multiuser DS-CDMA", *IEEE Wireless Communications and Networking Conference, WCNC2003*, New Orleans, Louisiana, March 16-20, 2003.